

THE X-RAY EMISSION OF M81 AND ITS NUCLEUS

G. FABBIANO

Harvard-Smithsonian Center for Astrophysics

Received 1987 April 14; accepted 1987 July 29

ABSTRACT

M81 was observed in X-ray with the imaging detectors on board the *Einstein Observatory*. The discovery of a pointlike nuclear source in its low-luminosity Seyfert nucleus was reported by Elvis and Van Speybroeck. Here we report the results of a complete spatial and spectral analysis of this galaxy and of its nuclear source. We detect nine individual sources in M81, including the one at the nucleus, with X-ray luminosities greater than $\sim 2 \times 10^{38}$ ergs s^{-1} , assuming a distance of 3.5 Mpc. Five of these are associated with the spiral arms, and three of them are associated with resolved thermal radio emission and/or giant H II regions. We also find that about two-thirds of the nonnuclear emission is not resolved in detected sources. The radial distribution of the X-ray surface brightness closely resembles that of the blue light, as found for other spiral galaxies. A comparison in different energy ranges of the total nonnuclear emission of M81 with that of M31 suggests a more active star formation history in M81. The X-ray sources detected in M81 are also more luminous than those of M31, but we cannot tell if this is due to an increased probability of X-ray source formation in M81 or also to a shift of the luminosity function of X-ray sources in this galaxy toward intrinsically higher luminosities.

The X-ray spectral data of the nuclear source are well fitted with a steep power-law spectrum with energy index $\alpha_E \sim 3$ and intrinsic absorption column $\sim 10^{21}$ – 10^{22} cm^{-2} . The fit to a thermal bremsstrahlung model is similarly good and gives a relatively low temperature $kT \sim 1$ keV. The soft spectrum of the nuclear source could be related to the soft spectral components seen in more luminous active nuclei. If we interpret this emission in terms of the accretion disk model of Czerny and Elvis and Bechtold *et al.*, we find a mass for the central compact object of $\leq 10^4$ – $10^5 M_\odot$ and accretion rates $\leq 10^{-4}$ – $10^{-3} M_\odot yr^{-1}$. The measured N_H is far less than those predicted from an extrapolation of the properties of brighter nuclei, suggesting that the explanation of the properties of active nuclei in terms of obscuration is not always applicable. The soft spectrum, if typical of low-luminosity active nuclei, also suggests that the contribution of these objects to the 2–10 keV X-ray background might be less than previously thought.

Subject headings: galaxies: individual (M81) — galaxies: nuclei — galaxies: X-rays

I. INTRODUCTION

The detailed study of the *Einstein* X-ray observations of nearby spiral galaxies has given us a different way to probe into the properties of these systems and to further our understanding of some of the open questions of “classical” galactic X-ray astronomy. The X-ray emission by no means dominates the energy output of a normal spiral galaxy, which is dominated by the stellar light in the optical and by the reprocessed stellar light in the far-infrared (Fig. 1). It is, however, more important than the radio emission in the total energy balance, and, as the radio emission, it allows us to study aspects of the astrophysical phenomena taking place in these systems which would not be otherwise accessible. In particular, while the radio emission allows us to study the magnetic fields of spiral galaxies and their content of energetic particles, the X-ray emission gives us a direct look at the evolved component of the stellar population, such as neutron stars and black holes. It also gives us the only tool for studying directly any hot gaseous component that may be present in these systems, as for example in the case of the starburst galaxies NGC 253 and M82 (Fabbiano and Trinchieri 1984; Watson, Stanger, and Griffiths 1984; Fabbiano 1988).

The *Einstein* observations of nearby spiral and irregular galaxies have revealed a number of bright discrete sources in these systems, possibly close accreting binaries similar to the Galactic X-ray sources, and also supernova remnants (e.g., Van Speybroeck *et al.* 1979; Long, Helfand, and Grabelsky 1981;

Long *et al.* 1981; Seward and Mitchell 1981; Fabbiano and Trinchieri 1984; Trinchieri, Fabbiano, and Palumbo 1985; Palumbo *et al.* 1985; Fabbiano and Trinchieri 1987). They have also shown at least three components of the X-ray source population, instead of the two found in the studies of the Milky Way (e.g., Van den Heuvel 1980): a bulge, a young Population I, and a disk component. They have revealed a close relationship between the blue-emitting stellar population and the general X-ray emission of spiral galaxies and a strong link of the X-ray emission with the radio continuum and possibly far-infrared emission (Fabbiano, Feigelson, and Zamorani 1982; Fabbiano, Trinchieri, and Macdonald 1984; Fabbiano and Trinchieri 1985; Palumbo *et al.* 1985; Fabbiano 1986; Fabbiano, Gioia, and Trinchieri 1988).

In this paper we report the results of the analysis of the X-ray observations of M81 with the *Einstein* satellite (Giacconi *et al.* 1979). M81 (NGC 3031) is a nearby ($D \sim 3.3$ – 5.75 Mpc; Bottinelli *et al.* 1984; Sandage 1984) early-type spiral galaxy with a prominent bulge and very well defined spiral arms. Because of its “grand design” appearance it has been the target of investigations aimed at testing and understanding galactic density waves (e.g., Roberts, Roberts, and Shu 1975; Visser 1980*a, b*; Bash and Visser 1981; Bash and Kaufman 1986). It has been well studied both in the optical and in the radio wavelengths (e.g., Schweizer 1976; Connolly *et al.* 1972; Beck, Klein, and Krause 1985; Kaufman *et al.* 1987). A large body of observations against which to discuss the X-ray results

X-RAY EMISSION OF M81

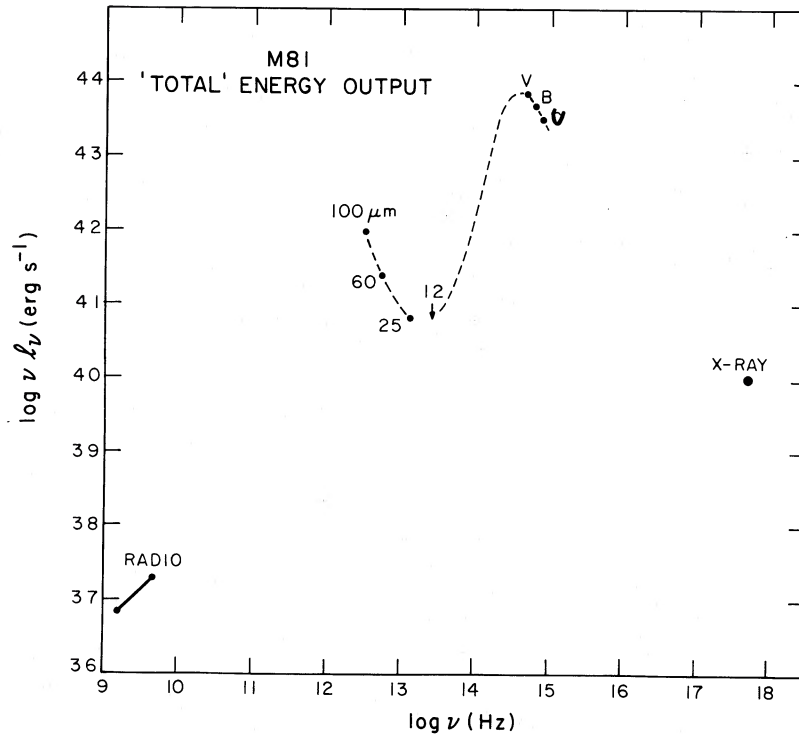


FIG. 1.—Energy distribution of the total emission of M81. Area below the $\log \nu L_\nu$ curve is proportional to the power emitted in each frequency band. Radio points are from Hummel (1980) and Beck, Klein, and Krause (1985) and include contribution of the nuclear source. This amounts to $\sim 37\%$ of the total emission at 4.7 GHz. Far-infrared points are from *Cataloged Galaxies in the IRAS Survey* (1985), and the optical points are from de Vaucouleurs, de Vaucouleurs, and Corwin (1976). The total X-ray 2 keV monochromatic luminosity is from the compilation of Fabbiano and Trinchieri (1985). It is consistent with the value given in Table 1 for the total X-ray luminosity of M81.

is therefore available. M81 is morphologically similar to M31, for which very deep X-ray observations also exist (Van Speybroeck *et al.* 1979; Long and Van Speybroeck 1983; Fabbiano, Trinchieri, and Van Speybroeck 1987), thus allowing a direct comparison of global emission properties and of the statistical properties of the X-ray source populations in two similar galaxies. M81 also hosts a low-luminosity Seyfert nucleus (Peimbert and Torres-Peimbert 1981; Shuder and Osterbrock 1981), whose X-ray detection has been reported and discussed

by Elvis and Van Speybroeck (1982). Here we report the results of a spectral analysis of this nucleus and we discuss its properties in the context of those of more active nuclei.

For ease of comparison, in this paper we adopt a distance of 3.5 Mpc for M81, which is consistent with the distance adopted in previous X-ray and radio studies (Elvis and Van Speybroeck 1982; Beck, Klein, and Krause 1985). We will discuss explicitly those instances in which a different choice of the distance would affect significantly our conclusions.

TABLE 1
THE EINSTEIN X-RAY OBSERVATIONS OF M81^a

Instrument	Sequence Number	Date	Time ^b (s)	Count Rate (counts s ⁻¹)	L_x (ergs s ⁻¹)
IPC	2102	1979 Apr 27	6515	0.24 ± 0.01^c	1.7×10^{40d}
HRI	585	1979 May 3 1979 Sep 27	28673	... ^e	... ^e

^a R.A. = $9^h 51^m 83^s$, decl. = $+69^\circ 18' 18''$, $D = 3.5$ Mpc.

^b The time is the effective live time for each observation.

^c The IPC count rate was calculated using the background-subtracted counts in the 0.2–3.5 keV band from a circle of $8'$ radius centered on the nucleus of M81. No X-ray emission associated with M81 is detectable outside this region. The background was subtracted using the standard background template (see text).

^d This is a 0.2–4.0 keV luminosity, calculated assuming a line of sight $N_H = 4.1 \times 10^{20}$ cm⁻² (Stark *et al.* 1984) and a thermal spectrum with $kT = 5$ keV. A multiplicative correction factor of 1.2 was applied to the IPC count rate to correct for mirror scattering and vignetting.

^e The HRI emission is almost all resolved into individual pointlike sources (see Table 2). The HRI field background does not allow the detection of diffused faint emission.

II. DATA ANALYSIS

The log of the observations used in this paper is given in Table 1 with the integrated count rates and luminosities measured by the IPC. The IPC field background was subtracted from the image to calculate the net source counts. This background was estimated from the templates produced by the *Einstein* reduction software and subtracted following the procedure described in Fabbiano and Trinchieri (1987; see also Trinchieri, Fabbiano, and Canizares 1986). The normalization of the background template calculated by the standard reduction software was used, since this background represents well the IPC surface-brightness profile in the source-free areas at large radii.

a) The X-Ray Contour Maps

Figures 2 and 3 show the IPC and HRI contour maps of M81, overlaid onto the blue (O) POSS plate. To obtain the

IPC maps we have used the broad-band (0.2–3.5 keV) background-subtracted image to optimize the statistics. No significant differences can be seen when comparing the maps from the soft (0.2–0.8 keV) and the hard (0.8–3.5 keV) bands. The significance levels of the contours are calculated using the original—non-background-subtracted—image to evaluate the statistical noise. The HRI field background was evaluated from an annulus of 240" and 420" inner and outer radii centered on the field center. This area is devoid of bright sources, and a radial profile of the HRI surface brightness shows that it is representative of the average flat-field background. The IPC data shown in the map of Figure 2 were averaged over 16" regions and smoothed with a Gaussian of $\sigma = 35''$. The HRI data (Fig. 3) were averaged over 8" regions and smoothed with a Gaussian of $\sigma = 10''$. The outermost contours in the maps represent the 2σ level above the average background level. We do not show the entire HRI field, but only the portion including M81. Source X-9 is therefore not visible in Figure 3.

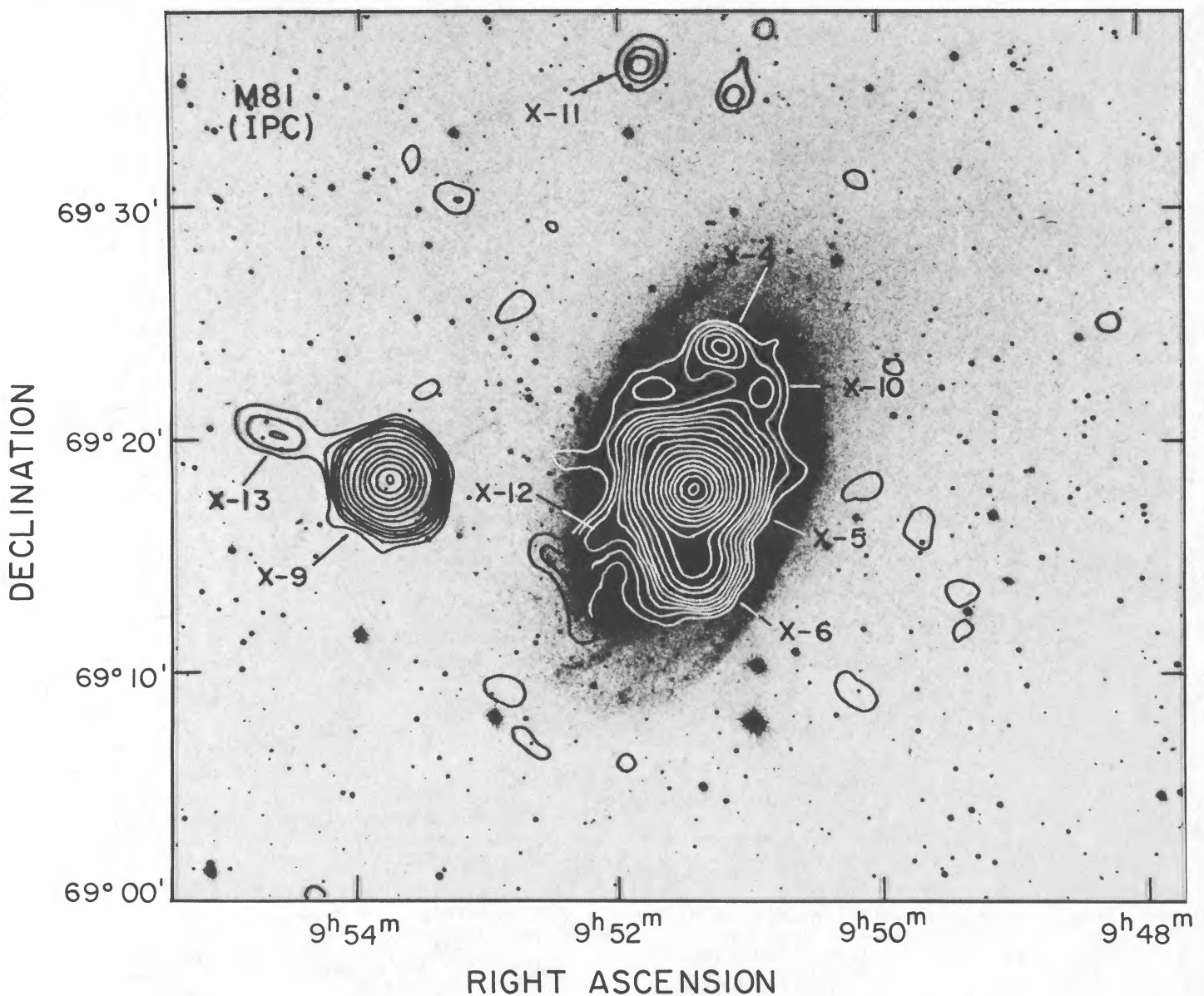


FIG. 2.—IPC contour map of M81 overlaid on the POSS O plate. The first contour is at 2σ above the field background. Discrete sources detected in the IPC image are indicated by an X followed by a number. Data were smoothed with a Gaussian with $\sigma_G = 35''$. The equivalent Gaussian sigma of a point source in this map is $\sigma_G \sim 57''$.

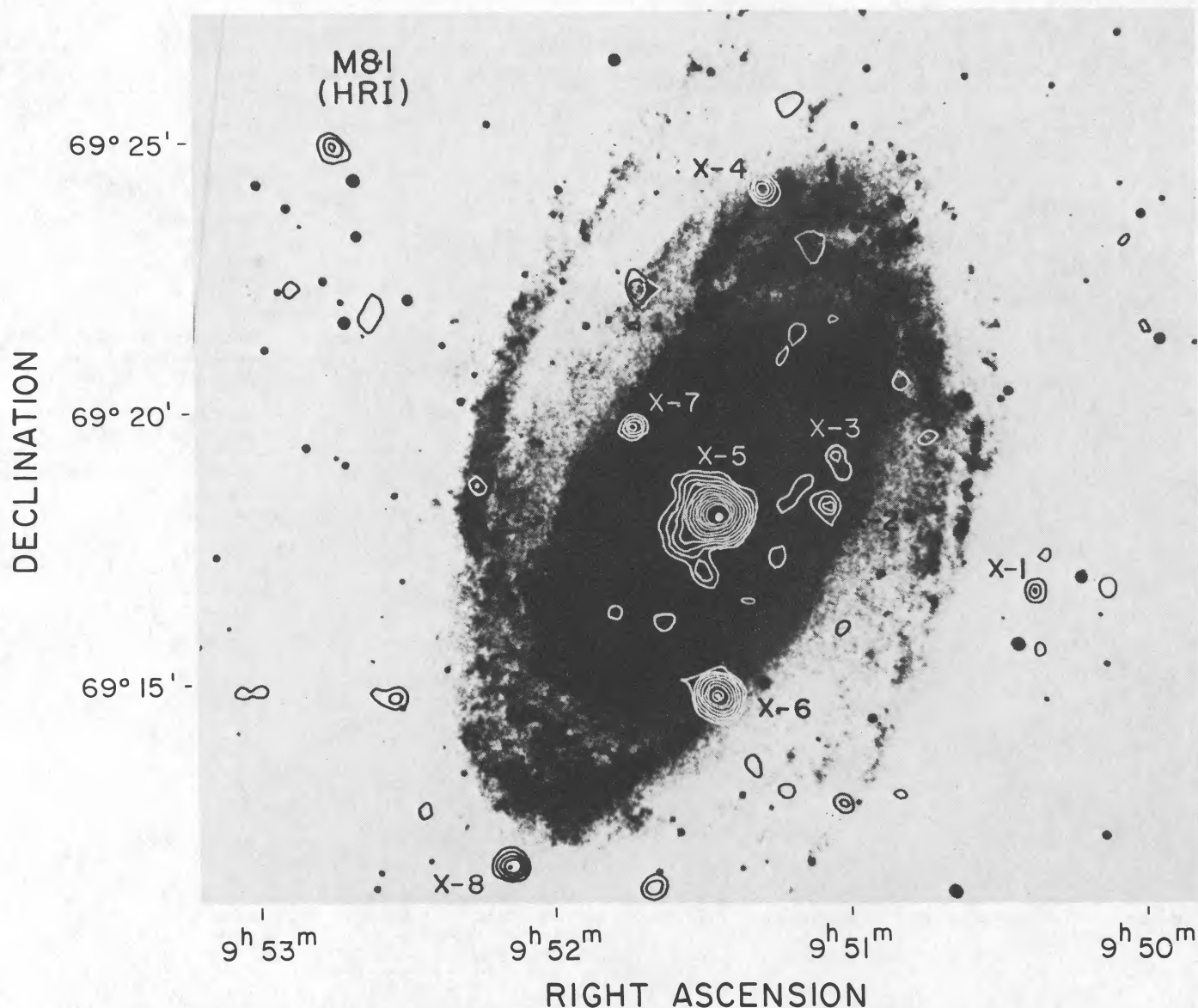


FIG. 3.—HRI contour map of M81 overlaid on POSS O plate. First contour is at 2σ above the field background. Discrete sources detected in the HRI image are indicated by an X followed by a number. For sources detected in both the IPC and the HRI fields the same number is used.

b) Fluxes and Luminosities of Separate Components

Several discrete sources are seen in the *Einstein* images of M81. Tables 2 and 3 list the resolved X-ray sources detected in the HRI and IPC observations of M81. The sources are listed in increasing right ascension order and are identified with an X-number. If a source has been detected in both imaging instruments, it has the same X-number in both the HRI and IPC lists. The X-numbers are also used in Figures 2 and 3 to identify sources.

i) HRI Sources

To evaluate the source counts in the HRI image, we cannot use the background estimated by the *Einstein* reduction software, since the presence in the field of the bright nuclear source causes spuriously high background levels (see *Einstein* Revised User's Manual [RUM]; Harris and Irwin 1984). We have therefore measured the field background as described above.

Nine sources are detected in the HRI image, one of which (X-9) is certainly not associated with M81. One of these detec-

tions, source X-3, is marginal, since the count rate diminishes when the counts are evaluated from the standard circle of $18''$ radius centered on the centroid rather than from the $12'' \times 12''$ detection box. Since we cannot derive the spectral parameters of each individual source, the fluxes quoted in Table 2 are all derived for the same spectral parameters: a galactic line of sight $N_H = 4.1 \times 10^{20} \text{ cm}^{-2}$ (Stark *et al.* 1984) and an equivalent temperature $kT = 5 \text{ keV}$. Standard corrections for scattering, coma, vignetting, and quantum efficiency (see RUM) were applied to the count rates to derive the fluxes. With this procedure we find that the two brightest sources in the field, the nucleus (X-5) and source X-9 outside M81, have comparable X-ray fluxes if their spectral parameters are not too different. The nucleus is the brightest source associated with M81, with an X-ray luminosity of $7.5 \times 10^{39} \text{ ergs s}^{-1}$. All the other sources possibly in the galaxy have luminosities ranging from 1.9×10^{38} to $1.4 \times 10^{39} \text{ ergs s}^{-1}$. If we use the best-fit parameters for a power-law model for the nuclear source (see below), we obtain a luminosity of $1.3 \times 10^{41} \text{ ergs s}^{-1}$ for this source.

TABLE 2
THE X-RAY SOURCES DETECTED IN THE HRI OBSERVATION OF M81^a

Source Number	R.A.	Decl.	Counts ^b ± Error	$f_x(0.2-4.0 \text{ keV})$ ($\text{ergs cm}^{-2} \text{ s}^{-1}$)	$L_x(0.2-4.0 \text{ keV})$ (ergs s^{-1})	Comments
1. (X-1).....	9 ^h 50 ^m 22 ^s .69	69°16'44".2	18.4 ± 7.7 (15.1 ± 4.6)	1.3 × 10 ⁻¹³	1.9 × 10 ³⁸	
2. (X-2).....	9 51 3.38	69 18 19.8	22.4 ± 8.0 (18.1 ± 4.9)	1.4 ± 10 ⁻¹³	2.1 × 10 ³⁸	Part of extended region?
3. (X-3).....	9 51 3.68	69 19 14.9	11.4 ± 7.3 (15.1 ± 4.6)	Marginal, part of extended region?
4. (X-4).....	9 51 17.60	69 24 9.1	28.4 ± 8.4	2.0 × 10 ⁻¹³	3.0 × 10 ³⁸	Also in IPC; bright star in M81 error circle?
5. (X-5).....	9 51 26.90	69 18 7.8	824.0 ± 29.4	5.1 × 10 ⁻¹² (9.1 × 10 ⁻¹¹)	7.5 × 10 ³⁹ (1.3 × 10 ⁴¹)	Nucleus; also in IPC using the IPC best-fit spectral parameters $\alpha_E = 3$ and $N_H = 4.8 \times 10^{21} \text{ cm}^{-2}$
6. (X-6).....	6 51 27.13	69 14 46.5	147.4 ± 13.7	9.5 ± 10 ⁻¹³	1.4 × 10 ³⁹	Also in IPC; coincident with radio emission (see Fig. 5)
7. (X-7).....	9 51 43.90	69 19 44.9	23.4 ± 8.1	1.5 × 10 ⁻¹³	2.2 × 10 ³⁸	Coincident with radio source No. 75 of Bash and Kaufman (1986)
8. (X-8).....	9 52 8.76	69 11 42.2	37.4 ± 8.9	2.8 × 10 ⁻¹³	4.1 × 10 ³⁸	Red faint object in error circle
9. (X-9).....	9 53 48.20	69 18 9.2	337.4 ± 19.5	3.5 × 10 ⁻¹²	...	Outside M81; also in IPC blue faint object in POSS plates near centroid

^a Assumed parameters: $N_H(\text{galactic}) = 4.1 \times 10^{20} \text{ cm}^{-2}$; $kT = 5 \text{ keV}$; $D = 3.5 \text{ Mpc}$.

^b The counts are from an 18" radius circle centered on the source centroid. This circle contains ~78% of the counts from a point source. The counts in parenthesis for sources 3, 5, and 7 are from the 12" × 12" detection cells.

TABLE 3
THE X-RAY SOURCES DETECTED IN THE IPC OBSERVATION OF M81^a

Source Number ^b	R.A.	Decl.	Counts ^c ± Error	$f_x(0.2-4 \text{ keV})$ ($\text{ergs cm}^{-2} \text{ s}^{-1}$)	$L_x(0.2-4 \text{ keV})$ (ergs s^{-1})	HR	Comments
1. (X-10).....	9 ^h 50 ^m 53 ^s	69°22'19"	13.8 ± 5.1 M	~1.2 × 10 ⁻¹³	~1.8 × 10 ³⁸	...	At 2.7 σ , only in the hard band (0.8–3.5 keV) giant H II region no. 138 of Kaufman <i>et al.</i> (1987) in error circle.
2. (X-4).....	9 51 14	69 24 18	29.3 ± 7.1 M	2.8 × 10 ⁻¹³	4.1 × 10 ³⁸	...	Also in HRI
3. (X-6).....	9 51 26	69 15 0	111.3 ± 16.9 L	9.8 × 10 ⁻¹³	1.5 × 10 ³⁹	0.46 ± 0.11	Also in HRI
4. (X-5).....	9 51 26	69 18 8	718.2 ± 28.5 ^d	5.9 × 10 ⁻¹² (1.1 × 10 ⁻¹⁰)	8.7 × 10 ³⁹ (1.6 × 10 ⁴¹)	0.09 ± 0.04	Nucleus; also in HRI using the IPC best-fit spectral parameters $\alpha_E = 3$ and $N_H = 4.8 \times 10^{21} \text{ cm}^{-2}$
5. (X-11).....	9 51 48	69 36 16	19.2 ± 6.0 M	2.2 × 10 ⁻¹³	Outside M81
6. (X-12).....	9 52 10	69 16 10	18.4 ± 6.1 M	1.6 × 10 ⁻¹³	2.4 × 10 ³⁸	...	Prominent H II region within error circle (no. 9 of Kaufman <i>et al.</i> 1987, also a 6 cm radio source)
7. (X-9).....	9 53 48	69 18 28	431.0 ± 21.2 M	4.1 × 10 ⁻¹²	...	0.28 ± 0.04	Outside M81; also in HRI
8. (X-13).....	9 54 38	69 20 25	19.1 ± 6.0 M	2.1 × 10 ⁻¹³	Outside M81

^a Assumed parameters: $N_H(\text{galactic}) = 4.1 \times 10^{20} \text{ cm}^{-2}$; $kT = 5 \text{ keV}$; $D = 3.5 \text{ Mpc}$.

^b The source number is sequential in Right Ascension, as for the HRI source list. The X-number denomination is the same as the one used for the HRI sources: i.e., the same source will have the same X-number, IPC sources not detected in the HRI are numbered starting from X-10.

^c An "L" or an "M" indicates if the source counts are from the "Local" DETECT or the "Map" DETECT program (see text). The counts are from the broad band (0.2–3.5 keV), except for source X-10.

^d The counts are from the MDETECT detection cell but the background was estimated locally from an annulus of 180" and 220" inner and outer radii (see text).

ii) *IPC Sources*

Table 3 lists eight sources detected in the IPC field. A ninth source, identified with M82, was at the edge of the IPC field of view and because of the motion of the satellite was visible only for a fraction of the observing time. Because of this we do not list it here. Three of these sources, X-9 (also detected in the HRI), X-11, and X-13 are a long way outside the optical image of M81 (see Fig. 2), and therefore are unlikely to be associated with it. The sources were not all detected by the same method. Background variations due to the bright central source and the unresolved galaxy emission caused problems for the innermost sources. For all the sources, except the nucleus (X-5) and the nearby source X-6, we give the net counts found by the “map-detect” program, which estimates the field background using a background template (Harnden *et al.* 1984). Source X-6 was only found by the “local-detect” program, which evaluates the background from a region immediately surrounding the $144'' \times 144''$ detection box. The nuclear source is in a region of local emission above the field background level, but it is also very bright and therefore source counts will dominate the region used by the “local-detect” to evaluate the background, resulting in a spuriously low source count rate. We have therefore used the raw counts from the detection cell and we have subtracted a background estimated locally from an annulus of $180''$ and $220''$ inner and outer radii. While being representative of the local M81 emission, this background does not include a significant contribution from the central source, which is contained within a $180''$ circle (see Fig. 7 below).

The IPC fluxes derived for sources X-4, X-5, X-6, and X-9 are consistent with the HRI fluxes for the same sources, indicating that they are neither very absorbed nor have very hard spectra. Only for three sources do the statistics allow us to derive meaningful hardness ratios (HR). These are defined as the difference between the net source counts in the IPC hard (0.8–3.5 keV) and soft (0.2–0.8 keV) bands, divided by the net counts in the broad (0.2–3.5 keV) band. They are listed in Table 3. We notice in particular that the HR of source X-9 is 0.28 ± 0.04 , indicating a harder spectrum for this bright source than for the nuclear source, which has $HR = 0.09 \pm 0.04$. This and their comparable brightness and proximity prevent the use of the MPC data to constrain the spectrum of the nucleus of M81 (see below).

iii) *Positions and Identifications*

The typical 90% uncertainties on the HRI source position, including the boresight error, are $\sim 4''$. Those on the IPC sources are $\sim 45''$. These are average values based on the comparison of the X-ray positions with the optical positions for the identifications of *Einstein* medium survey sources (I. M. Gioia 1987, private communication). Figure 4 is an accurate overlay of the X-ray source positions and error circles on the optical plate of M81 from Sandage (1961). It shows relatively bright objects within the positional errors of sources X-2, X-4, and X-8. The object in the X-2 circle cannot be resolved in the POSS plates because of the bright diffuse emission of M81. The object in the X-4 circle is of similar brightness in the red (E) and blue (O) POSS plates, while that in the X-8 circle seems relatively brighter in the red. Their magnitudes are comparable or slightly brighter than those of the brightest stars in M81 (~ 19 mag; see Sandage 1984). Without further information we cannot comment on the likelihood of these objects being the counterparts of the X-ray sources or just chance superpositions. Within the error circle of source X-12 is a prominent

H II region (No. 9 of Kaufman *et al.* 1987, also a 6 cm radio source) and another giant H II region is adjacent to the error circle of source X-10. Sources X-7 and X-6 are also near or on the spiral arms.

Figure 5 shows the X-ray source positions and error circles superposed on the VLA 1.4 GHz map of Bash and Kaufman (1986). The inner edges of the spiral arms are sketched on the figure for reference. Four of the sources are associated with radio features: these are the nuclear source (X-5), source X-6, source X-7, and possibly the IPC source X-10. Source X-7 is coincident with source 75 of Bash and Kaufman, which, according to these authors, could be related with the nuclear activity. This source is nonthermal and is not associated with H α emission (M. Kaufman 1987, private communication; Kaufman *et al.* 1987). An H II region, No. 221 of Kaufman *et al.*, is also near X-7 and is coincident with the radio source shown in Figure 5 to the east of the X-ray position. The association of X-7 with this object is however unlikely, given the accuracy of the HRI positions. The radio source within the error box of X-10 is the giant H II region of 138 of Kaufman *et al.* (1987). These authors notice that this region is likely to contain a supernova remnant. The X-ray luminosity of X-10 is much larger than those of supernova remnants in the Milky Way ($L_X \sim 10^{33-37}$ ergs s $^{-1}$; e.g., Gorenstein and Tucker 1974) and also extreme for the bright remnants in the LMC (Long, Helfand, and Grabelski 1981). It is therefore unlikely that we are detecting the X-ray emission of the supernova remnant in region 138. A more likely counterpart for the X-ray source would be a young massive binary system, possibly in the giant H II region. None of the X-ray sources is associated with background radio sources (indicated with numbers in the figure). Source X-4 is close to the background source 53, but the HRI box is small enough to exclude the possibility of an identification.

Inspection of the POSS plates at the positions of the three sources outside the optical body of M81 (X-9, X-11, and X-13) reveals a possible counterpart only for X-9, where a faint blue object is visible near the X-ray centroid. This source is also near the Dwarf Magellanic Galaxy, No. 66 of Van den Bergh (1959) (also Holmberg IX). However, the positional differences, and the expected X-ray flux (see Fabbiano and Trinchieri 1985) of this faint galaxy ($B = 14.3$; Bertola and Maffei 1974), both exclude an identification with source X-9.

iv) *Search for Variability*

We have performed a preliminary search for variability of the detected sources, by applying a χ^2 test for the hypothesis of consistency with a mean value to the light curves of time-binned data. We have applied this method to the nuclear source in both IPC and HRI observation, and to sources X-4 and X-6 in the IPC observation. We find marginal indication of possible variability in time scales of the order of a few minutes in a few instances. We show in Figure 6 the most promising stretch of data from the IPC observation of the nuclear source, for which we obtained a reduced $\chi^2 = 2.28$ for 13 degrees of freedom, corresponding to a probability of chance occurrence of $\sim 1\%$. Similar results are found for portions of the observations of sources X-4 and X-6.

c) *The Radial Distribution of the X-Ray Surface Brightness*

Figure 7a shows two radial profiles of the X-ray surface brightness of M81, derived from the background-subtracted (0.2–3.5 keV) IPC image. The “minor axis” profile was derived

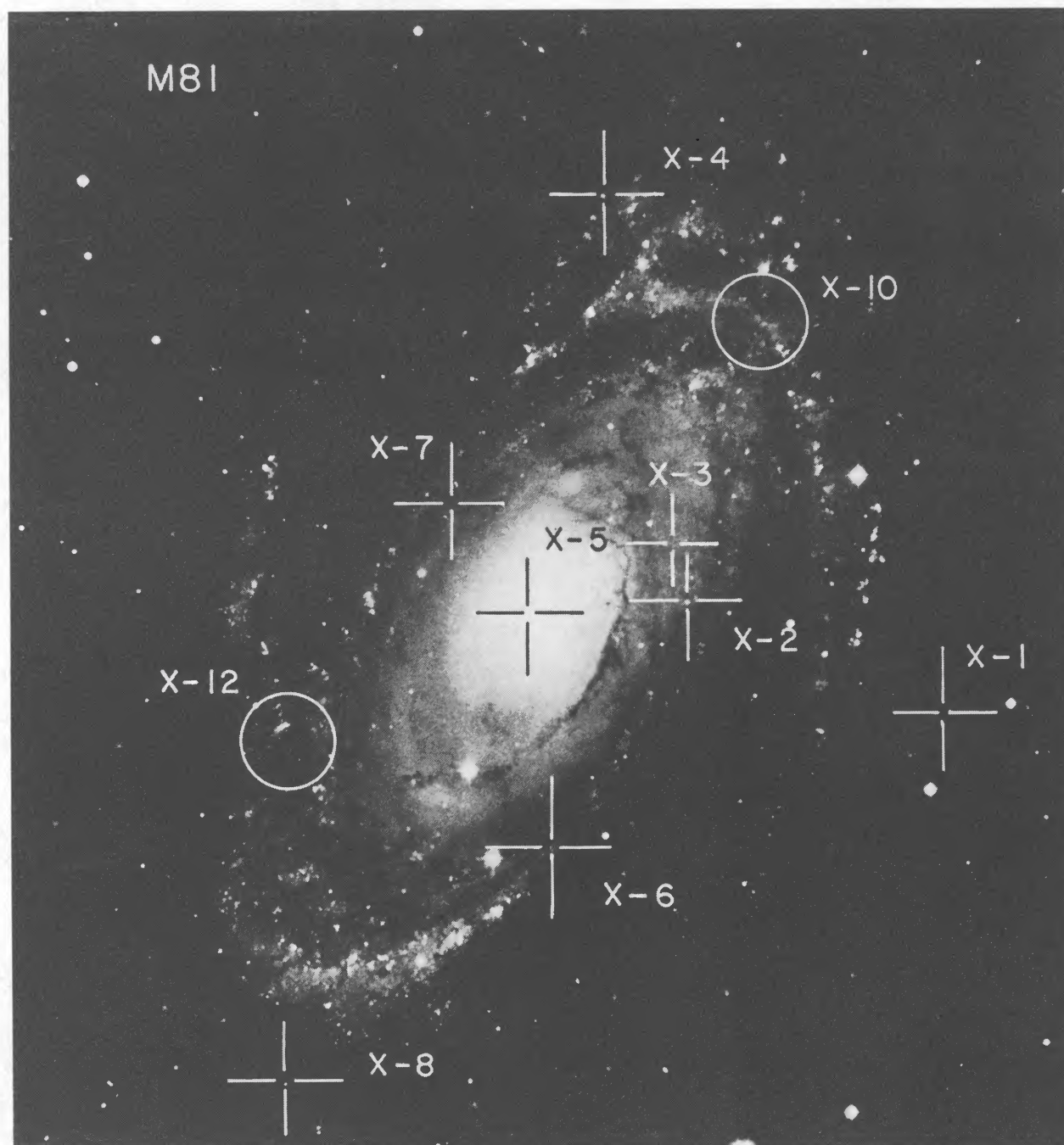


FIG. 4.—Overlay of the X-ray source positions and error circles on the plate from Sandage 1961. This overlay was done using the POSS O plate as a reference. The regions within the crosses represent the error regions of the HRI sources (90% positional uncertainties $\sim 4''$), the larger circles are the error regions for the IPC sources (90% positional uncertainties $\sim 45''$). Whenever possible, the more accurate HRI positions were used.

from two 40° pie-shaped sections centered on position angles 80° and 260° , with the data binned in circular annular sectors $20''$ wide. The “major axis” profile was derived in a similar way from the complementary parts of the image. Superposed on the surface brightness profiles of Figure 7a we also show a Gaussian of $\sigma = 50''$, to represent the IPC point response function for a soft spectrum source (Mauche and Gorenstein 1986). As discussed in the next section, the nucleus of M81 has a soft X-ray spectrum. This Gaussian represents well the “minor axis” profile, which is clearly dominated by the nuclear source, except perhaps in the last couple of points. The “major axis” profile instead gradually declines out to $\sim 8'$ from the nucleus.

Beyond this radius no X-ray emission is detected. In Figure 7a, source X-6 can be clearly identified and dominates the surface brightness profile between $140''$ and $240''$.

In Figure 7b is shown a composite profile, in which the high-resolution HRI data have been used in the inner $150''$ region. These data were binned in circular annuli around the centroid of the nuclear source and were then matched to the IPC profile. The IPC profile shown in this figure is the “major axis” profile of Figure 7a, except that between $140''$ and $240''$ only the data from the northern sector were used, to exclude source X-6. Since source X-6 was not included in this profile, its shape is truly indicative of the average integrated emission

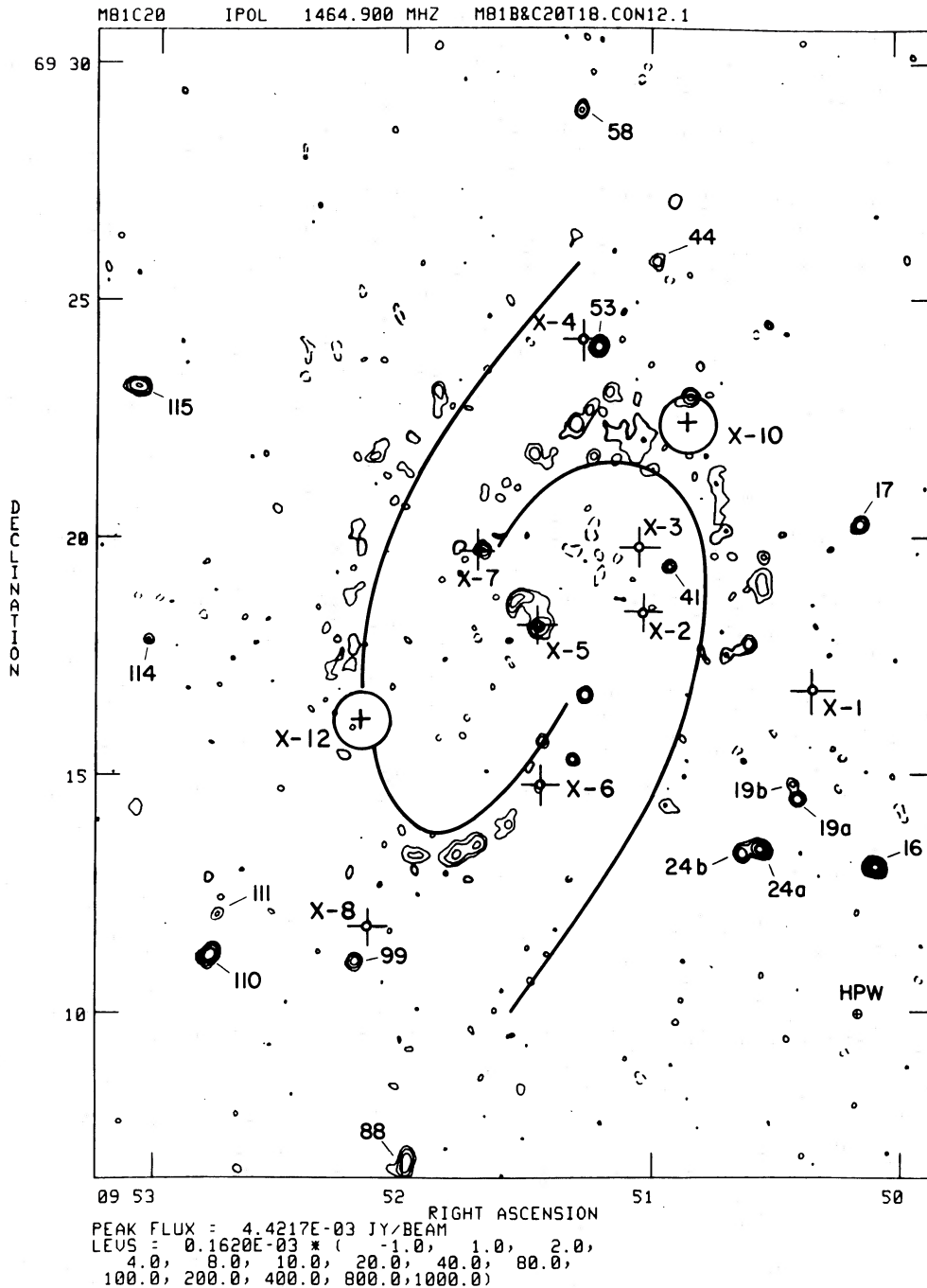


FIG. 5.—X-ray source positions overlaid on the 1.4 GHz map of Bash and Kaufman (1986). Inner edges of the spiral arms are sketched for reference

of the disk/arms of M81. The HRI point response function is drawn on the nuclear source profile and is a good representation of the data within $\sim 40''$ (see insert in Fig. 7b). The emission outside $60''$ from the center is not dominated by the nuclear source and is definitely extended. Divergences from a pointlike distribution are also suggested by the outermost contours of source X-5 in the HRI contour map of Figure 3.

This profile is compared with the optical and radio continuum profiles (as reported by Beck, Klein, and Krause 1985) in Figure 8. It follows rather well the optical profile, as has already been seen in the case of other spiral galaxies (M83,

Trinchieri, Fabbiano, and Palumbo 1985; M51, Palumbo *et al.* 1985; M33, Trinchieri, Fabbiano, and Peres 1987; and possibly NGC 6946, Fabbiano and Trinchieri 1987). It is not easy to compare it with the radio continuum profile of Beck, Klein, and Krause (1985), because the latter was derived from a map obtained with a $2.45'$ beam from which the central bright nuclear source had been subtracted. It is probably therefore quite uncertain in the inner $3'$ region. Unfortunately the sensitivity of the X-ray observation does not allow us to follow the surface brightness distribution in the outer regions, where it would be more meaningful to compare the two profiles.

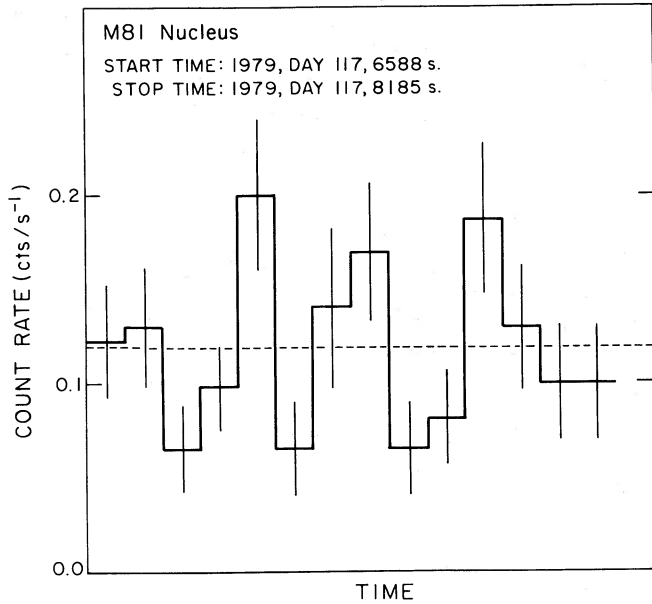


FIG. 6.—Light curve of a portion of the IPC data of the nuclear source (X-5). Data are binned in 122 s bins.

d) Spectral Analysis

We have performed spectral fits of the IPC data to thermal bremsstrahlung and/or power-law spectra with low-energy-absorption cutoffs using the procedures described in Fabbiano and Trinchieri (1987). These are based on the calibrations of Harnden *et al.* (1984) and Fabricant and Gorenstein (1983).

i) The Nuclear Source

M81 has an active nuclear X-ray source (Elvis and Van Speybroeck 1982). We have therefore fitted the data from the central point source (X-5) with both an absorbed power-law spectrum, typical of active nuclei (e.g., Mushotzky *et al.* 1980) and with an absorbed thermal bremsstrahlung (exponential plus Gaunt) spectrum. Since this source wandered off the central calibrated area of the IPC field that can be used for the spectral analysis of point sources, we only used those portions of the observation when the source falls in the calibrated part of the field. This results in a 35% reduction of the exposure time on the nuclear source. The source counts to be used in the spectral analysis were taken from a $180''$ circle centered on the centroid of source X-5, and the background counts were estimated from the surrounding annulus of $300''$ and $360''$ inner and outer radii.

Source X-6 is situated $201''$ south of the nuclear source (using the more accurate HRI positions) and is a factor of ~ 5.4 – 6 fainter than the nucleus, for the same assumed spectrum. Given the IPC point response function and the position of the two sources, we estimate that less than 30% of X-6 counts will be included in the circle used to estimate the source counts of X-5. This means that X-6 will contribute at the most 5% of the counts used for the spectral analysis. Similarly, the three fainter sources X-2, X-3, and X-7 will contribute no more than $\sim 2\%$ of the spectral counts. It is difficult to estimate the amount of unresolved bulge emission included in the spectral analysis. However, the HRI and IPC fluxes, which originate from different-sized regions, are very close (Tables 2 and 3), and exclude the dominance of a diffuse bulge component. We are therefore confident that the results of the spectral fitting of the

IPC data so derived are representative of the spectral properties of the nucleus of M81. As an *a posteriori* argument, the results of this spectral fitting reported below are totally uncharacteristic of the average spectral properties of the “normal” emission of spiral galaxies, which tend to have rather hard spectra (e.g., Fabbiano and Trinchieri 1987; see also Fabbiano, Trinchieri, and Van Speybroeck 1987 for the bulge of M31). The details of the spectral fits and the results are summarized in Table 4. Data from the IPC Pulse Height Analyzer channels 2–12 were included in the fit. The uncertainties on the spectral parameters given in Table 4 are all at the 90% confidence level for two interesting parameters. The 68%, 90%, and 99% confidence regions for the spectral parameters, the raw spectral data and the best-fit spectra are shown in Figure 9. The power law and the exponential plus Gaunt best-fit χ^2 are equally good. The IPC data are fitted well with either steep power laws or with a very cool thermal source. In both cases the intrinsic absorption is above the line-of-sight value.

We find that the spectral parameters derived by Elvis and Van Speybroeck for this source, using the HRI and MPC data (energy index $\alpha_E = 1.4$, $N_H = 1 \times 10^{22}$) are well outside the 99% IPC confidence contour. This discrepancy is easily understandable since a sizable fraction of the MPC counts ($\sim 30\%$), is likely to be due to source X-9, resulting in an artificially higher flux in the harder energy channels, if these counts are all attributed to the nucleus of M81. Source X-9 (Table 3) has an IPC flux comparable to that of the nuclear source X-5, and it is also harder. This implies that it could contribute relatively more of the MPC counts than the nuclear source. Source X-9 is situated only $13'$ from the center of the field of view, where the MPC response is $\sim 80\%$. Also at least $\sim 40\%$ of the emission within the inner $7'$ circle is due to nonnuclear sources and possible unresolved emission in M81. Elvis and Van Speybroeck worried about possible contamination of the MPC count rate by the neighboring galaxy M82, but neglected the effect of the bright source X-9 and of the nonnuclear galactic emission of M81.

Since we cannot use the MPC data to better constrain the spectral parameters of the nuclear source, as in the case of the bulge of M31 and of the nucleus of M33 (Fabbiano, Trinchieri, and Van Speybroeck 1987; Trinchieri, Fabbiano, and Peres 1988), we have tried a joint fit of the HRI and IPC data of this source with the IoA (Cambridge) spectral fitting software developed by R. Shafer and adapted to the *Einstein* instru-

TABLE 4
RESULTS OF THE SPECTRAL FITS

Fit	N_H (cm^{-2})	α_E^b or kT (keV)	χ^2	ν
A. Source X-5 (Nucleus), IPC Time = 4262 s ^a				
IPC power law	$(4.8^{+7.8}_{-3.8}) \times 10^{21}$	$\alpha_E = 3.0^{+2.0}_{-1.5}$	5.6	8
IPC thermal	$(1.2^{+2.8}_{-0.6}) \times 10^{21}$	$kT = 1.1^{+1.1}_{-0.5}$	5.5	8
IPC + HRI power law	$(6.2^{+3.8}_{-3.8}) \times 10^{21}$	$\alpha_E = 3.7^{+2.3}_{-1.7}$	7.4	9
IPC + HRI thermal	$(3.2^{+1.0}_{-2.0}) \times 10^{21}$	$kT = 0.6^{+0.7}_{-1.0}$	7.6	9
B. M81 (Galaxy, Nucleus excluded), IPC Time = 6515 s ^c				
IPC thermal	$< 10^{22}$	$kT = > 0.4$	7.9	6

^a IPC source radii, $0''$ – $180''$; IPC background radii, $300''$ – $360''$; IPC net counts in fit, 745.6 ± 31.7 .

^b α_E is the energy spectral index, defined as $f_\nu \propto \nu^{-\alpha_E}$.

^c IPC source radii, $200''$ – $500''$; IPC background radii, $500''$ – $600''$; IPC net counts in fit, 355.5 ± 45.1 .

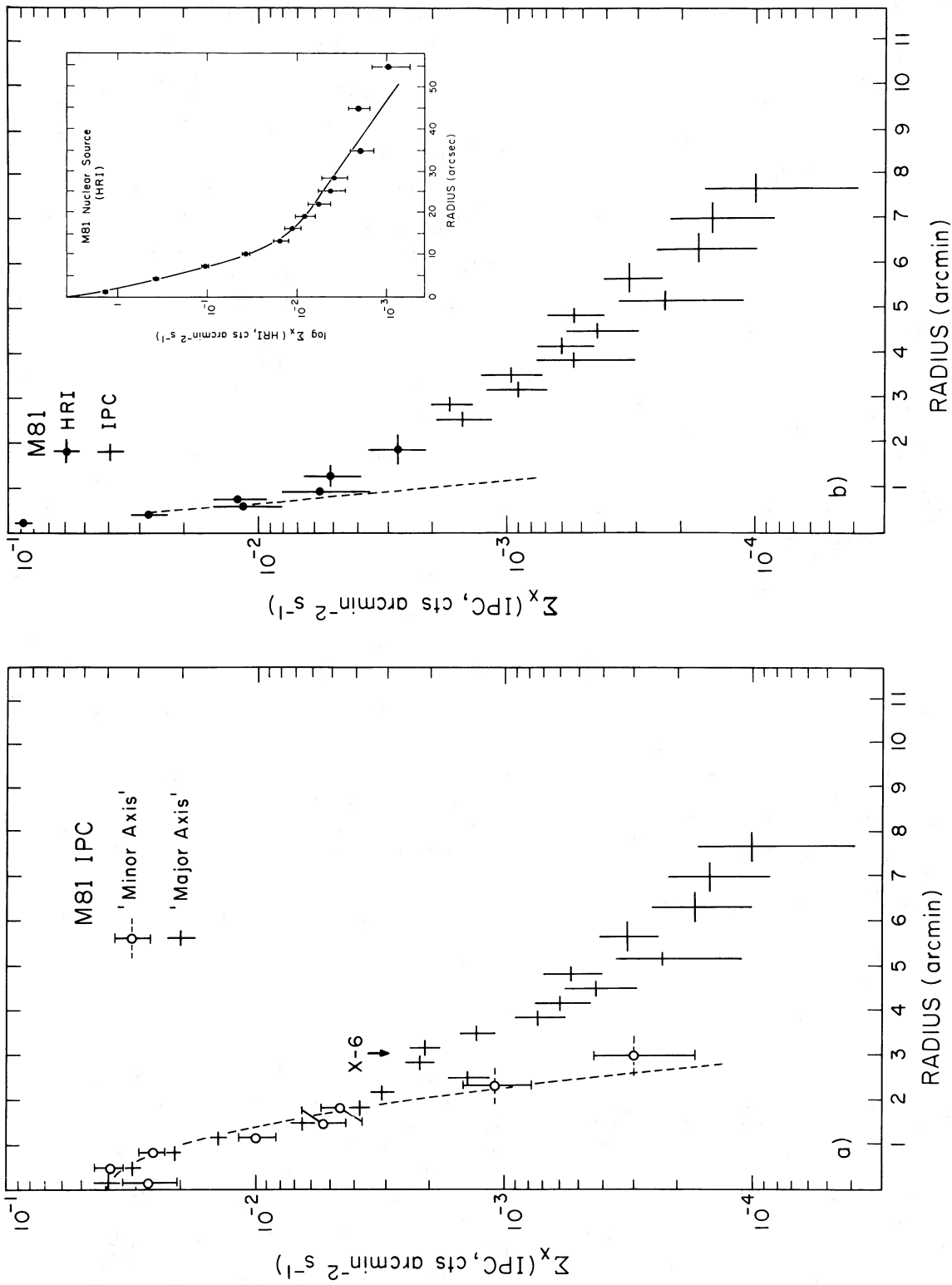


Fig. 7.—(a) "Minor" and "major" axis IPC X-ray surface-brightness profiles of M81 (see text). The IPC point response function is plotted on the nuclear source profile. (b) Composite HRI and IPC major axis profile. The bright source X-6 was subtracted from the data. The HRI point source response is also plotted. A higher resolution radial profile of the nuclear source is shown in the insert together with the HRI point response.

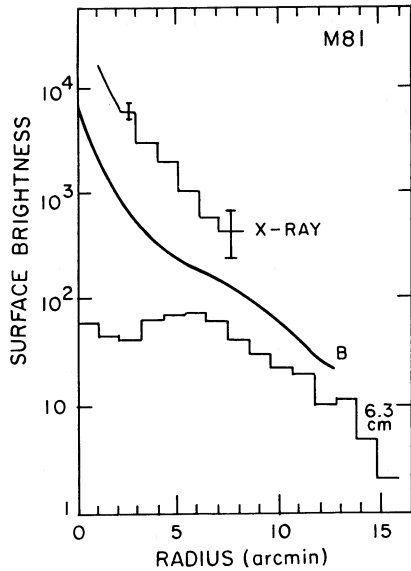


FIG. 8.—X-ray, optical and radio continuum (4.75 GHz) radial profiles of M81. Optical and radio profiles are from the compilation of Beck, Klein, and Krause (1985). Bright compact nuclear source was subtracted from the radio data.

ments by K. Arnaud (K. Arnaud 1987, private communication). To do this fit we have added a 10% error to the statistical error of the HRI counts, to account for systematic uncertainties in the relative calibration of the two instruments. These fits require higher values of N_H than do the IPC fits. The results are given in Table 4 and the confidence contours are shown in Figure 9 as dashed lines.

ii) The "Galactic" Emission of M81

To estimate the spectral parameters of the nonnuclear emission of M81, we have performed a spectral analysis of the background-subtracted counts from a region between 200" and 500" from the nucleus. The azimuthally averaged radial profile of M81 shows that no significant emission can be detected outside this radius (Fig. 7). The background was estimated from a surrounding annulus 100" wide. We have fitted these data with an absorbed thermal spectrum. The results (Table 4 and Fig. 10) show that the spectral parameters are poorly constrained. The confidence regions are consistent with a purely galactic line-of-sight absorption column, as was found for other spiral galaxies by Fabbiano and Trinchieri (1987).

III. DISCUSSION

a) The X-Ray Emission of M81

Including the nuclear source, nine discrete X-ray sources are detected associated with the optical body of M81. We can ask several questions about the X-ray properties of this galaxy: are these point sources likely to be in M81, or could they be chance superpositions? What is their nature? Do they account for all of the X-ray emission of M81? How does M81 compare with other spiral galaxies for which X-ray data of similar or better quality exists? How do the X-ray properties of M81 relate to its emission in other different wavelengths? In the following we will examine these points and we will summarize what can be inferred from the X-ray observations of M81.

i) The Nature of the Resolved Sources

Although firm identifications are not presently available, for statistical reasons most, if not all, of the sources detected in

M81 are likely to be associated with this galaxy. Based on the results of the *Einstein* medium survey (Gioia *et al.* 1984), in fact, we would expect ~ 2 serendipitous sources to be detected in 1 deg^2 of sky at the flux limit of our observations, while nine sources are instead detected in the area covered by M81, which amounts to $\sim 0.04 \text{ deg}^2$. As discussed in § IIb(iii), one is associated with the nucleus (see also Elvis and Van Speybroeck 1982), and we will discuss it in detail later. Five sources are associated with the spiral arms, and three of them are associated with resolved thermal radio emission and/or giant H II regions. The likely counterparts of these objects therefore belong to the very young Population I. Given their luminosities of the order of or above a few $10^{38} \text{ ergs s}^{-1}$, these sources are likely to be very close binary systems composed of an early-type star and a compact evolved object. Variability, if confirmed, would support this hypothesis.

Sources X-1, X-2, and X-3 are instead not associated with the spiral arms and could therefore be low-mass binary systems belonging to the older disk Population I. This type of X-ray sources are responsible for a large fraction of the X-ray emission of the Milky Way and possibly of other spiral galaxies (see Fabbiano 1986, and references therein).

ii) Resolved Sources and Total Emission

To estimate how much of the X-ray luminosity of M81 cannot be accounted for by resolved sources, we have compared the total IPC luminosity of this galaxy (Table 1) with the total luminosity attributable to point sources, both IPC and HRI (Tables 2 and 3). We find that the integrated galaxy luminosity is $\sim 1.7 \times 10^{40} \text{ ergs s}^{-1}$, while the total point source contribution, including the nucleus, amounts to $\sim 1.1 \times 10^{40} \text{ ergs s}^{-1}$, resulting in $\sim 35\%$ of the total emission due to unresolved or diffuse sources. The fraction goes up to $\sim 67\%$ if the nuclear source is not included.

Since the same spectral parameters were used in calculating the luminosities of the various components, the above estimate is really an estimate of the percentage of detected counts not attributable to individual sources above the detection threshold, corresponding to a source luminosity of $\sim 2 \times 10^{38} \text{ ergs s}^{-1}$ for the same spectral parameters. A source of uncertainty in these estimates is the correction to be given to the integrated luminosity of M81 because of flux scattered outside of the detection circle. The correction assumed in Table 1 is rather conservative, but we can calculate a still more conservative estimate of the "diffuse" fraction of the X-ray emission by not applying any correction to the total galaxy counts. In this case we obtain $\geq 22\%$ and $\geq 51\%$ for the fraction of the total and nonnuclear emission, respectively, not attributable to detected sources. Therefore at least half of the nonnuclear emission of M81 is due to either the integrated contribution of individual sources below the detection threshold or to diffuse emission. Figure 8 shows that the radial distribution of this emission component largely follows that of the starlight.

A comparison with other spiral galaxies which have been studied in detail in X-rays suggests that this emission is largely due to fainter single sources. Figure 11 in particular shows a plot of the unresolved/diffuse fraction of the galaxies' nonnuclear emission versus the detection threshold for individual sources for five galaxies: M81, M33 (Trinchieri, Fabbiano, and Peres 1987), M83 (Trinchieri, Fabbiano, and Palumbo 1985), NGC 253 (Fabbiano and Trinchieri 1984) and M51 (Palumbo *et al.* 1985). The diffuse/unresolved fractions of M33, M83, NGC 253, and M51 were estimated from the published data.

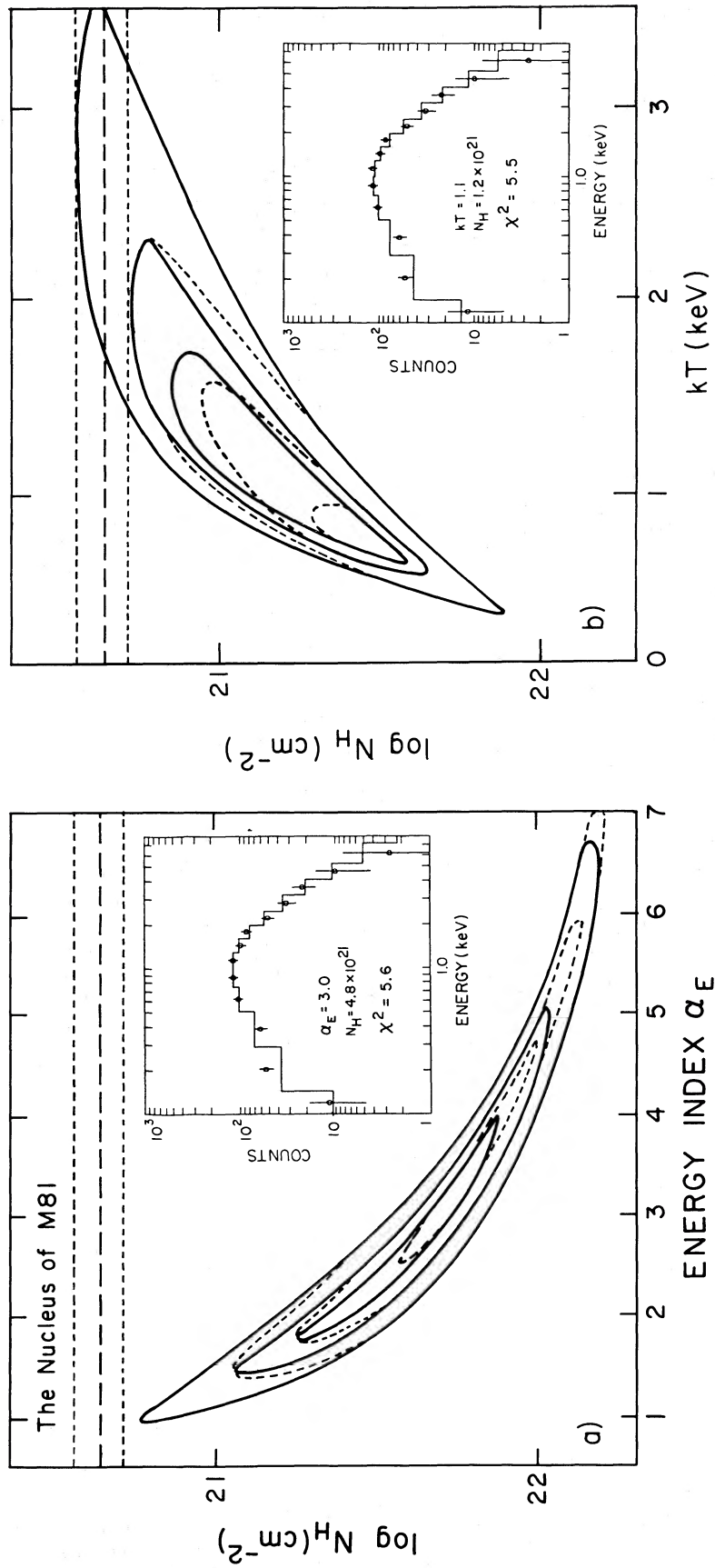


FIG. 9.—The 68%, 90%, and 99% two-parameter confidence contours for spectral fit of the nuclear source (X-5). Solid lines are from the IPC data alone, dashed lines are from the joint IPC and HRI fit. Dotted horizontal lines represent the line of sight N_H (Stark *et al.* 1984); dashed horizontal lines represent the 90% confidence bounds on N_H (see Elvis *et al.* 1986). (a) Absorbed power-fit; (b) absorbed exponential plus Gaunt fit. IPC observed spectral counts and the best-fit spectra convolved with mirror and IPC response are shown in the insets.

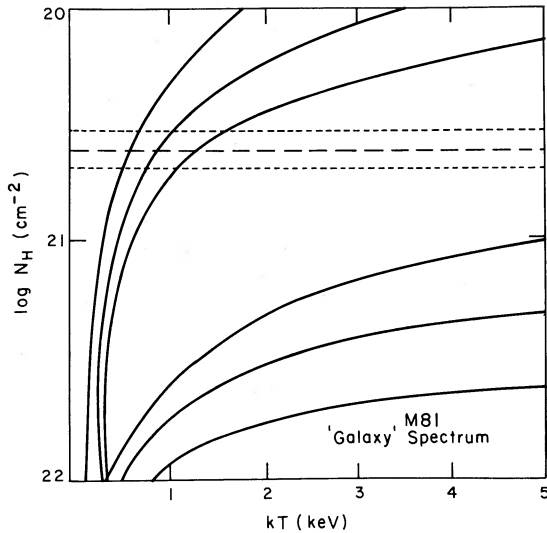


FIG. 10.—The 68%, 90%, and 99% two-parameter confidence contours for absorbed exponential plus Gaunt fit of the nonnuclear IPC M81 data. Dotted horizontal lines represent the line of sight N_H (Stark *et al.* 1984) and the dashed horizontal lines represent the 90% confidence bounds on N_H (see Elvis *et al.* 1986).

Although these estimates are quite uncertain for the reasons discussed above in the case of M81, a clear trend toward more of the galaxy's luminosity being resolved into individual sources, when the detection luminosity threshold is lower, is evident in Figure 11. This is what we would expect if the unresolved-diffuse emission is indeed due to the integrated contribution of sources below the detection threshold.

M31 is not included in this comparison because an *Einstein* measurement of its integrated X-ray luminosity is not available. Van Speybroeck *et al.* (1979), however, remarked that the sum of the luminosities of the individual sources detected in this galaxy approaches the global values measured with previous nonimaging X-ray satellites and that in this case most of the X-ray emission can be accounted for by individual sources. Since the threshold luminosity for an individual source in this galaxy is between 10^{36} and 10^{37} ergs s^{-1} , M31 would be in agreement with the trend shown in Figure 11.

In principle, in the absence of confusion effects that will lower the single source detection efficiency in crowded areas, the slope of the distribution of points in Figure 11 could be used to get an idea of the power-law slope of the luminosity

function of single X-ray sources in spiral galaxies. For a power-law differential luminosity function $dN/dl = Cl^\alpha$ with $-2 < \alpha < 0$, where N is the number of sources of luminosity l , the "diffuse" nonnuclear fraction of the galaxy emission will be proportional to $l_{th}^{2+\alpha}$, where l_{th} is the threshold luminosity for a given observation. The slope of the differential luminosity function α can then be derived by subtracting 2 from the slope of the line describing the distribution of points in Figure 11. The data points suggest a fairly flat distribution, with slope possibly < 1 . This could be the effect of a steep luminosity function of the X-ray sources in a galaxy, with power-law exponent $\alpha < -1$. However, only five galaxies are plotted, and moreover they are of different morphological types. Also, confusion effects can modify the slope, acting in two opposite ways. The diffuse percentage would tend to increase, but the luminosity threshold would also increase because of the increased background level. A definition of the slope of the average luminosity function of sources in spiral galaxies will have to wait for more sensitive observations of a better defined and larger sample.

iii) Comparison with M31

1. *Global properties.*—M81 and M31 are both early-type spiral galaxies with prominent bulges and fairly well defined spiral arms. They are both classified as Sb by Sandage and Tamman (1981), while de Vaucouleurs, de Vaucouleurs, and Corwin (1976) classify the former as Sab and the latter as Sb. Both galaxies have been studied extensively at different wavelengths, and the *Einstein* observations of M31 (Van Speybroeck *et al.* 1979; Long and Van Speybroeck 1983; Fabbiano, Trinchieri, and Van Speybroeck 1987) offer the most detailed close view of an early-type spiral galaxy in X-rays. They offer then a unique opportunity for comparing the different global emission properties of galaxies of similar morphology and for a detailed comparison of their resolved X-ray source component.

Beck, Klein, and Krause (1985) noticed that the 4.8 GHz radio luminosity of M81, excluding the contribution from the bright nuclear source, is approximately a factor of 2 larger than that of M31 (Berkhuijsen, Wielebinski, and Beck 1983), although its optical luminosity is only half that of M31 (Sandage and Tamman 1981). If instead we use the 1.4 GHz nonnuclear flux densities of Hummel (1980) for the two galaxies, we find similar radio powers. This would suggest a steeper radio spectrum for M31 (with spectral index $\alpha \sim -1$ to ~ -0.8) than for M81 ($\alpha = -0.64 \pm 0.03$; Beck, Klein, and Krause 1985).

It therefore appears that M81 is either more efficient than

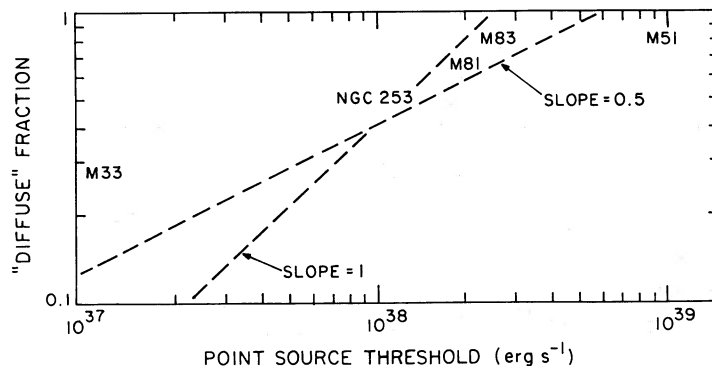


FIG. 11.—Unresolved/diffuse fraction of the nonnuclear emission of five spiral galaxies plotted in log-log plot vs. the threshold luminosity for point source detection.

M31 at accelerating electrons to high energies or that it has a considerably stronger thermal radio emission. The latter possibility, however, cannot explain totally the discrepancy at 4.8 GHz because thermal emission cannot be responsible for more than 30% of the emission of M81 at this frequency (Beck, Klein, and Krause 1985). Both galaxies have strong shock fronts in the context of the density wave theory (Roberts, Roberts, and Shu 1975) and the greater alignment of the magnetic field of M31 with the spiral arms suggests stronger shocks in this galaxy (Beck, Klein, and Krause 1985). It is therefore unlikely that the stronger radio emission of M81 is connected with acceleration of relativistic electrons in the spiral shocks, as suggested for NGC 3310 by Duric (1986), because in this case one would expect M31 to be the more powerful radio emitter, unless turbulence considerably reduces the polarization.

Connections between the radio continuum emission of spiral galaxies and their X-ray and far-infrared emission have been suggested (Fabbiano and Trinchieri 1985; Palumbo *et al.* 1985; Helou, Soifer, and Rowan-Robinson 1985; de Jong *et al.* 1985; Fabbiano, Gioia, and Trinchieri 1987). It is therefore meaningful to extend the comparison of the global emission properties of these two galaxies to include the X-ray and far-infrared luminosities. We use the X-ray luminosity of M31 listed in Long and Van Speybroeck (1983), which is $\sim 3.6 \times 10^{39}$ ergs s^{-1} , and we derive a far-infrared luminosity of 4.0×10^{42} ergs s^{-1} for this galaxy from the *IRAS* flux quoted by Helou, Soifer, and Rowan-Robinson (1985). We derive a far-infrared luminosity of 4.4×10^{42} ergs s^{-1} for M81 using the 100 and 60 μm flux densities of the “*IRAS* small-scale structure catalog” and the expression given in Persson and Helou (1987). We find that the nonnuclear X-ray emission of M81 ($L_x \sim 8-9 \times 10^{39}$ ergs s^{-1}) is a factor of 2–3 higher than that of M31 (this galaxy does not have a prominent nuclear source; Van Speybroeck *et al.* 1979). Its far-infrared luminosity instead is comparable with that of M31. Therefore relative to their optical emission, (and therefore independent of the distance estimates), M81 is overluminous by comparable amounts in the radio 4.8 GHz and X-ray emission. It is also overluminous, but to a lesser amount, in the far-infrared. The nuclear contribution to the far-infrared is only a few percent of the total emission. The nuclear emission at 100 μm is ~ 3 Jy (Rickard and Harvey 1984), while the total emission measured in the *IRAS* survey at the same wavelength is ~ 25 Jy.

These results are consistent with a connection between the radio, X-ray, and far-infrared emission (see Fabbiano, Gioia, and Trinchieri 1987). They point to a difference in the star formation history of M81 and M31, which has led to a more efficient production of X-ray, radio, and far-infrared sources in the former. The comparable excess luminosity of M81 in the radio continuum and the X-rays in particular is consistent with either mechanism suggested to explain the strong correlation observed between these two variables in the sample of spiral galaxies observed with the *Einstein* satellite (Fabbiano and Trinchieri 1985). It would be consistent with either a direct contribution of the binary X-ray sources to the acceleration of relativistic electrons (e.g., Cyg X-3, Samorski, and Stamm 1983; SS 433, Hjellming and Johnston 1981; Watson *et al.* 1983) or with a scenario involving a supernova stage in their evolution.

It is not clear why star formation should be more efficient in M81, if stronger spiral wave shocks are present in M31 (see above). A possibility would be that the gas supply in M31 may have been depleted by past more active star formation (e.g.,

Roberts, Roberts, and Shu 1975). Alternatively, the alignment of the magnetic field might not be a good indicator of the strength of the shocks.

2. *The luminosity function of arm/disk Population I X-ray sources.*—As can be seen from Figures 2, 3, and 4, the X-ray sources detected in M81 are associated with the galaxy’s disk and spiral arms. In M31, $\sim 33\%$ of the emission is due to bulge sources found within the inner 2' from the nucleus (Van Speybroeck *et al.* 1979). This would correspond to $\sim 23''$ at the distance of M81. A similar component in M81 would not be detectable with the *Einstein* instruments, because of the strong nuclear source (see § IIc). In the following we will then compare the X-ray sources resolved in M81 with the “Pop I” sources of M31, i.e., those sources not associated with the inner bulge or with globular clusters.

As discussed above, M81 (nucleus excluded) is $\sim 4-6$ times more luminous than M31 in X-rays relative to their optical luminosities. Therefore the question arises if this “excess” X-ray emission of M81 is due to a larger number of X-ray sources or if the X-ray sources in M81 are on the average more luminous than those in M31. In Figure 12 we plot the log of the number of these sources in luminosity bins against the log of the source luminosity (from Long and Van Speybroeck 1983). We also plot the luminosity distribution of the M81 sources. These sources are all more luminous than those detected in M31. The threshold for point source detection in M81 is

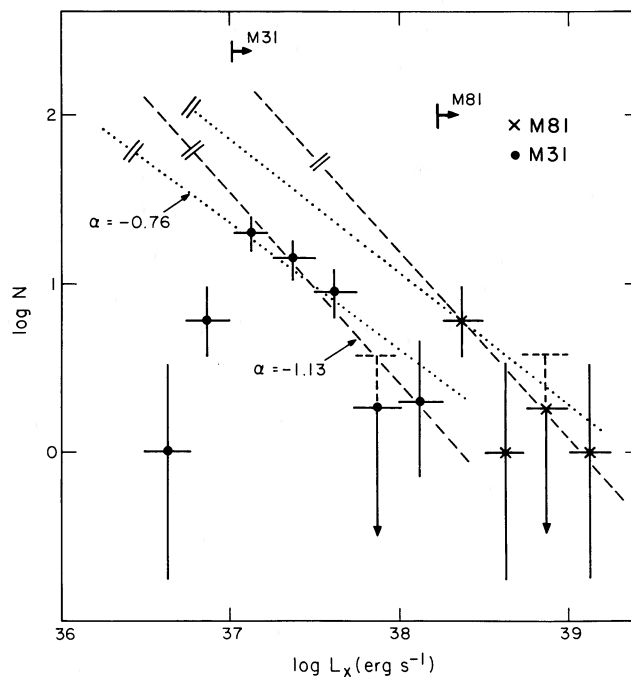


FIG. 12.—Log-log plot of the number of individual X-ray sources of a certain X-ray luminosity vs. the luminosity for M31 (dots, data from Long and Van Speybroeck 1983) and M81 (crosses). The completeness limits for the two galaxies are indicated by the horizontal arrows. The error bars on the points are at the 1σ level and were calculated using either a Gaussian error distribution or Poisson statistics when appropriate (Gehrels 1986). The dashed upper limits are at the 2σ level. Dotted and dashed lines represent two power-law approximations to the differential luminosity function of X-ray sources in M31. The lines crossing them at the low-luminosity end represent the points at which the luminosity function must turn off to avoid exceeding the total X-ray luminosity of M31. The same power laws are normalized to the M81 source distribution.

$\sim 2 \times 10^{38}$ ergs s^{-1} , higher than the most luminous M31 source. Only if the distance of M81 were as low as ~ 1 Mpc, would the luminosities of the point sources in M81 be consistent with those of the bright sources of M31. This is highly unlikely. A recent distance estimate by Sandage (1984) put M81 at 5.75 Mpc. At this distance the resolved sources would be ~ 2.7 times more luminous than in Tables 2 and 3. If the bright sources of M81 are accreting binary systems, their X-ray luminosities put them at or just above the Eddington luminosity for a $1 M_{\odot}$ object. This in itself however does not imply that there is an intrinsic difference between the X-ray sources of M81 and M31, because even if only the X-ray source production per unit optical luminosity were larger in M81, we would expect to see a small number of more luminous and therefore rarer X-ray sources in this galaxy.

The sample of the M31 X-ray sources is complete for $L_x > 10^{37}$ ergs s^{-1} (Long and Van Speybroeck 1983). Therefore, above this limit the sample can be used to define a luminosity function. The decrease in source counts observed below this limit can, at least in part, be due to incompleteness. Although the statistical significance of the points does not allow us to define a unique luminosity function, this can be represented by power laws in the range of those plotted in Figure 12 as dotted and dashed lines. The double lines crossing these power laws at the low luminosity ends represent approximate turn-off points. They were calculated under the assumption that the "Pop I" sources are responsible for $\sim 56\%$ of the X-ray luminosity of M31 (Van Speybroeck *et al.* 1979), by integrating the different power-law luminosity functions until the total "Pop I" luminosity was reached. Although the uncertainties are large, the turn-off point in M31 is probably at source luminosities between 10^{36} and 10^{37} ergs s^{-1} .

Assuming that a similar range of power laws can represent the luminosity function of the X-ray sources in M81, we can perform a similar calculation for this galaxy. We find (see Fig. 12) that in the case of flatter power laws ($\alpha \sim -0.7$ – -0.8) the turn-off point could be consistent with that of M31. For steeper power laws ($\alpha \sim -1.1$; as may be suggested by Fig. 11, see § IIIa[ii]) instead the turn-off point could occur at source luminosities ~ 10 times larger. However, the turn-off luminosity depends also on the normalization of the power-law model and this is now rather arbitrary. With the present data therefore we cannot definitely establish whether M81 simply has more X-ray sources than M31 or if these sources are instead more powerful on average. The quality of the data does not warrant more accurate calculations. If these galaxies could be observed with 10 times more sensitivity for point source detection, the above question could be answered.

b) The Nuclear Source

The main result of this work relative to the properties of the nuclear source of M81 is that its X-ray spectrum is very soft, with energy index $\alpha_E > 2$ ($f_{\nu} \propto \nu^{-\alpha_E}$), and is intrinsically absorbed, with $N_H \sim 10^{21}$ – 10^{22} cm^{-2} (see Table 4). The source could be variable in a time scale of a few minutes, however, the evidence of variability is very marginal and needs to be confirmed.

i) Comparison with the Bright Active Nuclei

Elvis and Van Speybroeck (1982) suggested that this X-ray source is a scaled-down version of the bright X-ray sources detected in Seyfert galaxies and QSOs. We can now extend this comparison to the spectral properties. Recent work both in the

Einstein energy range and encompassing the general emission spectrum of active nuclei (Elvis, Wilkes, and Tananbaum 1985; Elvis *et al.* 1986; Bechtold *et al.* 1987; Wilkes and Elvis 1987; Ward *et al.* 1987; Carleton *et al.* 1987) has in fact given a fairly clear picture of the energy distribution of these objects. We can therefore see if the nucleus of M81 has the general spectral characteristics of an active nucleus and if there is any relationship between the intensity of the nuclear source and its spectrum, which could suggest differences in the emission mechanisms at play.

1. *The radio through X-ray energy distribution.*—Figure 13 shows the radio to X-ray energy distribution of the nuclear source in a νf_{ν} plot. The radio flux densities were taken to be 100 mJy with a flat spectrum (Bartel *et al.* 1982); the millimeter and 10 μm points are from the catalog of Gezari, Schmitz, and Lee (1984); the 100 μm and 50 μm points are from Rickard and Harvey (1984); and the UV point is from the dereddened spectrum of Bruzual, Peimbert, and Torres-Peimbert (1982). The latter is strictly speaking an upper limit to the emission of the active nuclear source since the optical-UV spectrum is dominated by the stellar emission (Bruzual, Peimbert, and Torres-Peimbert 1982; Ellis, Gondhalekar, and Efstathiou 1982). The 10 μm point is from a small 3/6 aperture. The 100 μm and 50 μm points were obtained with a 50" aperture, but the comparable energy emitted in these two bands (Fig. 13) excludes a dominant galactic contribution (see Fig. 1).

In the same figure we plot for comparison similar energy distributions for a radio-loud active nucleus (3C 273) and for a radio-quiet active nucleus (Mrk 509), taken from Elvis, Czerny, and Wilkes (1987). The IR through X-ray energy distribution of the nucleus of M81 (see also Bruzual, Peimbert, and Torres-Peimbert 1982) is certainly consistent with those of the other two objects shown. A flat distribution in this type of plot is indeed typical of bright active nuclei (Carleton *et al.* 1987). In contrast the radio emission of the nucleus of M81 is intermediate between those of the radio-loud and the radio-quiet nuclei, relative to the other parts of the continuum shown in the figure. The X-ray spectra of 3C 273 and Mrk 509 are different from that of the nucleus of M81. However, soft components can be present in the spectra of bright active nuclei (e.g., Elvis, Wilkes, and Tananbaum 1985). We will discuss this more below.

From Figure 13a we can also exclude nonthermal mechanisms for the X-ray emission of the nucleus of M81, connected with the presence of a compact radio source. The radio flux is much lower than the X-ray flux, thus ruling out the possibility of a synchrotron-self-Compton explanation for the X-ray source. Also, the possibility that the steep X-ray spectrum is the exponential cut-off of the radio synchrotron emission is ruled out, since in this case one should see a dominant non-thermal UV emission, in excess of the measured UV flux, as can be seen by extending the radio power law.

2. *The steep spectral slope: comparison with PG1211+143 and an accretion disk model.*—The similarity of the general energy distribution of the nucleus of M81 with those of bright active nuclei reinforces the suggestion of this source being such an object (Elvis and Van Speybroeck 1982) and makes it meaningful to pursue further comparisons. Although the X-ray spectrum of active nuclei was generally believed to be represented by a power law with average energy index $\alpha_E \sim 0.7$ (Mushotzky 1984) the *Einstein* observations have shown the presence of softer emission components in these objects (Elvis, Wilkes, and Tananbaum 1985; Wilkes and Elvis 1987). A very

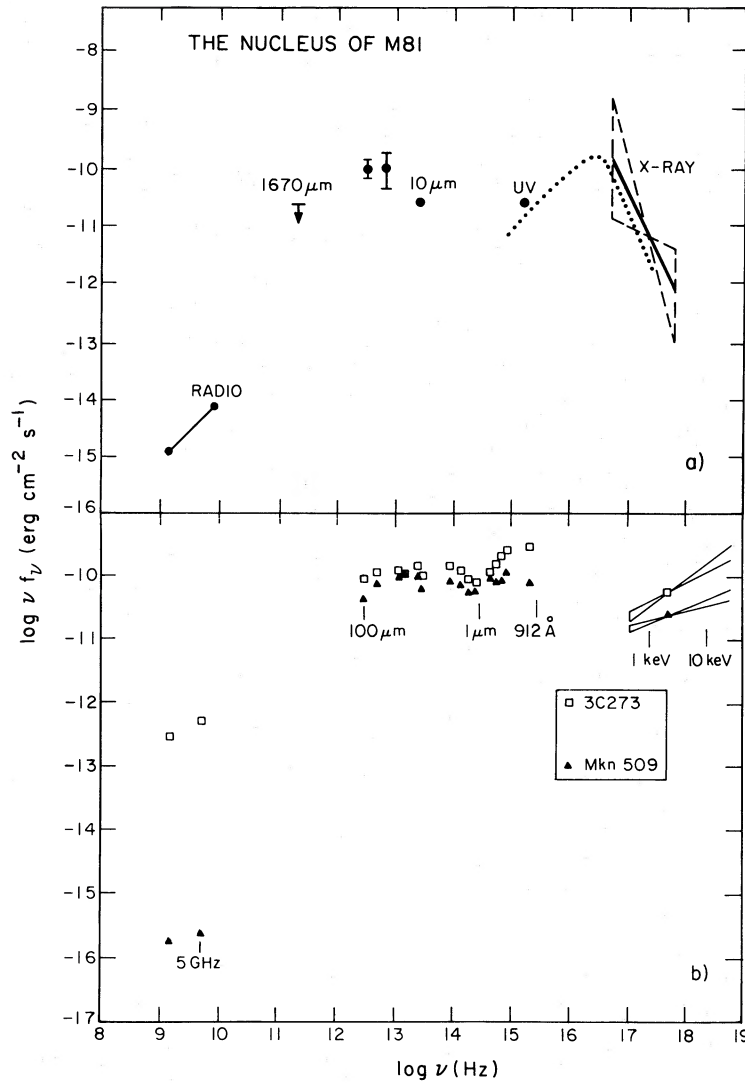


FIG. 13.—(a) Spectral continuum distribution from the radio to the X-rays for the nuclear source of M81 in a $\log \nu f_\nu$ vs. $\log \nu$ plot. The radio points are for a ~ 100 mJy flat spectrum source (Bartel *et al.* 1982; Crane, Guifrida, and Carlson 1976). The 1.6 mm and 10 μm points are from the compilation of Gezari, Schmitz, and Lee (1984), the 100 μm and 50 μm points are from Rickard and Harvey (1984), and the UV points is from Bruzual, Peimbert, and Torres-Peimbert 1982). The X-ray “butterfly” represents the range of spectral values allowed at the 90% confidence by the power-law fit of the IPC data. The curve joining the UV and X-ray regions represents the accretion disk model of Bechtold *et al.* (1987; see text). (b) Spectral continua of typical radio-quiet and radio-loud active nuclei are shown for comparison (from Elvis, Czerny, and Wilkes 1986).

clear example is the QSO PG1211+143 (Bechtold *et al.* 1987), where the *Einstein* spectrum is fitted by two components: a soft steep power law with $\alpha_E = 2.0(+1.0, -0.5)$ and a flatter power law with $\alpha_E < 1.2$ at the higher energies. The spectral index of the nucleus of M81 is at least as steep as that of the soft component of PG 1211+143. Our data do not require the presence of a flatter high-energy component, although a low-luminosity one could be present. X-ray imaging at higher energies will be needed to explore this point further.

Bechtold *et al.* suggested that the soft X-ray component of PG 1211+143 could be explained with emission from the inner regions of an accretion disk surrounding a central black hole and modeled the entire optical/UV to X-ray spectrum of this QSO under the hypothesis that a single accretion disk component could also account for the rising UV spectrum. Plotted in Figure 13 is the accretion disk model B of Bechtold *et al.*, scaled in flux to match the energy distribution of the

nucleus of M81. If a soft XUV spectral component is present in the nucleus of M81, the problem of an adequate reservoir of ionizing photons would be solved. In the absence of this component there would be at least a factor of 2 less photons than needed to explain the optical emission lines (Bruzual, Peimbert, and Torres-Peimbert 1982).

We can apply this model of a thin accretion disk (see also Czerny and Elvis 1987) to the nucleus of M81 to get an estimate of the mass of the central accreting object (M) and of the accretion rate (\dot{M}) in this framework. Using equation 6 of Bechtold *et al.* we can estimate a line in the M and \dot{M} plane (Fig. 14) representing the allowed values for M81, based on the flux emitted by such an accretion disk in the UV. To do this we use the dereddened nuclear flux at 1700 \AA of Bruzual, Peimbert, and Torres-Peimbert (1982). Since no clear evidence of a nonthermal UV component in the nucleus of M81 was found (Bruzual, Peimbert, and Torres-Peimbert 1982), this line

should really be considered an upper limit and is plotted as such in Figure 14.

We can further restrict the range of allowed M and \dot{M} by using the information that the X-ray spectrum of the nucleus of M81 has a steep slope similar to that of PG 1211+143 and that therefore the accretion disk will have to peak at similar frequencies. The lines relative to acceptable frequencies for PG 1211+143 are also plotted (*dashed line*) in Figure 14. The range of masses and accretion rates allowed by this model for the nucleus of M81 are $M \leq 10^4\text{--}10^5 M_\odot$ and $\dot{M} \leq 10^{-4}\text{--}10^{-3} M_\odot \text{ yr}^{-1}$, roughly $\sim 10^3$ and 10^5 times less respectively than those required for PG 1211+143. The dotted line in Figure 14 represents the locus of M and \dot{M} for which the system will radiate at the Eddington luminosity. The values of M and \dot{M} for the nucleus of M81 are such that the emission is sub-Eddington and therefore the model thin disk approximation is valid, unlike the case of PG 1211+143 (see Bechtold *et al.* 1987). A possible problem for this picture would be the presence of variability on time scales of a few minutes, if this is real. In this case the disk would be so viscous as to behave virtually as a solid body (Czerny and Czerny 1986). However, small scale variability in short time scales might not be a problem if the accretion disk has a hot corona, in which case variability might be connected with local phenomena. The dynamical time scale for our model accretion disk would be of the order of a few minutes (M. Elvis 1987, private communication).

3. *The absorbing column: comparison with the obscuration picture of active nuclei.*—The above discussion was based on the general emission properties of the nuclear source and on its steep spectral slope. Our results on the absorption column seen in this source can also be used to compare it with the results found for brighter active nuclei. Table 4 shows that the X-ray equivalent hydrogen column is in the range $N_{\text{H}} \sim 2 \times 10^{21}\text{--}1 \times 10^{22} \text{ cm}^{-2}$. These columns are larger, although consistent at the lower limit with the column derived from the UV $E(B-V) = 0.19$ of Bruzual, Peimbert, and Torres-Peimbert (1982), which corresponds to $N_{\text{H}} \sim 1.5 \times 10^{21}$ (Jenkins and Savage 1974).

A relationship between the 2–10 keV luminosity of active nuclei and the presence of absorption in their spectra led to the suggestion of Lawrence and Elvis (1982) of large amounts of dust near or in the broad-line emission regions in fainter nuclei, which could also explain the prevalent occurrence of Seyfert type 2 optical spectra in these objects. More recent data have shown that, while the relationship between hard X-ray luminosity and absorption is still statistically true, there are low-luminosity objects that are not heavily absorbed (see Elvis and Lawrence 1985 and references therein).

The properties of the nucleus of M81 clearly demonstrate that the obscuration picture is not always applicable. We cannot measure the 2–10 keV luminosity of this source, but based on our results we can safely assume that it is $< 10^{40}\text{--}10^{41} \text{ ergs s}^{-1}$. At these luminosities absorption columns $\sim 10^{23} \text{ cm}^{-2}$ or larger should be present in the extrapolation of the luminous nuclei results. Our spectral results instead set an upper limit of a few 10^{22} cm^{-2} to the absorption column, consistent with the values measured in the brightest objects. Although one cannot completely exclude a particular combination of the spatial distribution and size of the obscuring clouds in the Lawrence and Elvis (1982) picture, that may result in a relatively low absorption, our result together with the new evidence compiled by Reichert *et al.* (1985) suggests a parallel sequence to the absorption picture, consisting of relatively dust free nuclei. The optical–emission-line spectra of this type of nuclei should not be a function of the nuclear luminosity. The Seyfert type 1.5 spectrum of the nucleus of M81 (Peimbert and Torres-Peimbert 1981) is consistent with this picture.

ii) Comparison with Other Low-Luminosity Nuclei

The analysis of the *Einstein* observations of normal spiral galaxies has revealed so far two other instances of pointlike, relatively bright nuclear sources for which spectral data are available. These sources are in M33 (Long *et al.* 1981; Markert and Rallis 1983; Trinchieri, Fabbiano, and Peres 1987) and in NGC 1313 (Fabbiano and Trinchieri 1987). The X-ray spectrum of the nucleus of M33 is fitted with a steep power law

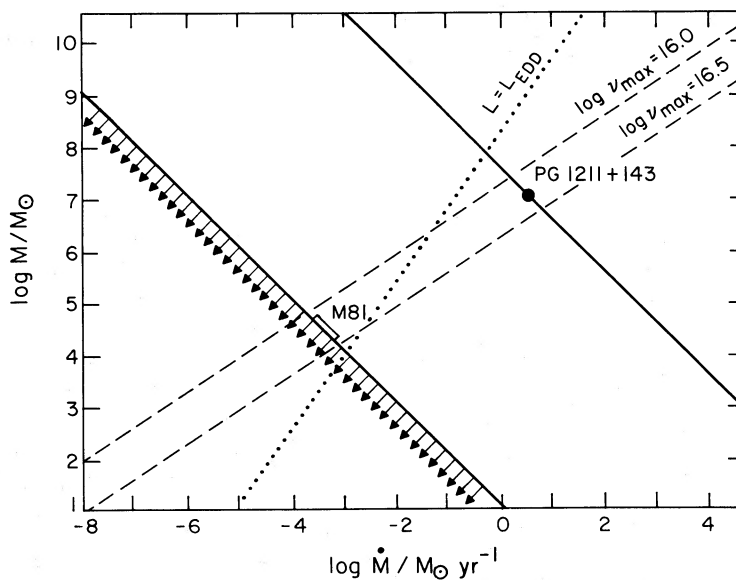


FIG. 14.—This is Fig. 6 of Bechtold *et al.* (1987) adapted to the nucleus of M81. This figure is explained in the text.

($\alpha_E \sim 1-2$), with intrinsic absorption (Trinchieri, Fabbiano, and Peres 1987). The spectral fit of the source in NGC 1313 definitely requires intrinsic absorption columns, in excess of the line of sight value. The data are also consistent with steep power-law spectra, but the statistics do not allow one to constrain this parameter usefully. Based on their X-ray spectral properties, these nuclear sources and the nucleus of M81 could then be similar objects.

However, the similarity stops here, since no sign of activity is present in the optical and radio data of M33 (e.g., O'Connell 1983; von Kappeler, Berkhuijsen, and Wielebinski 1978), and similarly no Seyfert-like lines are visible in the optical spectrum of NGC 1313 (J. Gallagher 1987, private communication). Although it is rather premature to reach firm conclusions based on only two objects, it cannot be excluded that these two nuclei represent a new type of source, possibly the radio-quiet counterpart of sources like that in the nucleus of 3C 264, which similarly shows no sign of optical activity (Elvis *et al.* 1981; Fabbiano *et al.* 1984). If this is so, it is quite appropriate for these sources to be found in spiral galaxies, in analogy with what is observed in radio-loud and radio-quiet optically active nuclei (Miller 1985 and references therein).

iii) Implications for the X-Ray Background

Following the discovery of the X-ray source in the nucleus of M81, Elvis, Soltan, and Keel (1984) derived a low luminosity X-ray luminosity function of active nuclei and calculated that the total contribution of the active nuclei to the 2–10 keV X-ray background would be $\sim 27\%$ (for $q_0 = 0.0$). More than half of this contribution would originate from sources with $L_x \sim 10^{40} - 10^{42.5}$ ergs s^{-1} . This luminosity function was not based on direct X-ray observations of low-luminosity active nuclei, but rather on relating the optical luminosity function of field galaxies of Kirschner, Oemler, and Schechter (1979) and the nuclear H α emission of a complete sample of spiral galaxies (Keel 1983) to the X-ray emission. This was done via a correlation between H α and X-ray emission measured in luminous active nuclei, which have rather hard X-ray spectra (Elvis *et al.* 1978; Kriss, Canizares, and Ricker 1980).

The soft X-ray spectrum of the nucleus of M81 introduces an additional source of uncertainty that must be taken into account in this type of calculation, which could result in a smaller contribution of the low-luminosity active nuclei to the X-ray background than estimated by Elvis, Soltan, and Keel. Most of their luminosity could be emitted in a softer energy range and their contribution to the 2–10 keV diffuse background could be quite small. On the other hand, we do not know how common and how bright the optically quiet X-ray active nuclei, such as those of M33 and NGC 1313, are. Their inclusion could raise the estimate of the contribution to the X-ray background, although their spectra suggest that even this type of source should contribute mainly in the soft energy range.

IV. CONCLUSIONS

The results of the analysis of the X-ray observations of M81 and their comparison with other relevant astrophysical objects and phenomena can be summarized as follows:

1. Excluding the nucleus, eight bright sources were detected in the *Einstein* images, with (0.2–4.0 keV) luminosities in excess of $\sim 2 \times 10^{38}$ ergs s^{-1} . Five of them could belong to the spiral arms and two could be marginally variable, suggesting that they are young massive accreting binary systems. The presence

of a bright pointlike nuclear source does not allow the detection of any X-ray inner bulge sources, similar to those present in M31 (Van Speybroeck *et al.* 1979). More than half of the nonnuclear X-ray emission is not resolved into individual sources. However the radial distribution of the X-ray surface brightness, which follows that of the starlight, and a comparison with other spiral galaxies suggest that this emission is likely to result from the integrated contribution of fainter discrete sources.

2. A comparison of M81 with the morphologically similar galaxy M31 shows that the former is overluminous in both the radio continuum and the X-ray emission and to a lesser extent the far-infrared emission, relative to their optical luminosity. These differences point to a difference in the star-formation history of the two galaxies, which has led to a more efficient production of X-ray, cosmic-ray, and far-infrared sources in M81. The comparable excess luminosity in the radio and the X-rays is consistent with the results of Fabbiano and Trinchieri (1985), which suggested a link between these two energy ranges. It is not clear why star formation should be more efficient in M81, since radio observations suggest that stronger spiral shocks are present in M31 (Beck, Klein, and Krause 1985). A possibility would be a depletion of the gas supply in M31 because of past, more active star formation (e.g., Roberts, Roberts, and Shu 1975).

3. The individual X-ray sources detected in M81 are all more luminous than the most luminous sources of M31. It is unlikely that this is due to an overestimate of the distance of M81. A comparison of the luminosity distribution of these sources with those of M31 shows that if the luminosity function of the X-ray sources in M81 is steep, then the function has a low-luminosity cutoff which is considerably higher than that in M31, and therefore the population of X-ray sources in M81 is intrinsically more luminous. The data do not rule out the possibility that the luminosity functions have the same slope and cutoff (but different normalizations) for both galaxies. In this case, the bright X-ray sources of M81 would only be the high-luminosity tip of a more numerous population of X-ray sources.

4. The nuclear source has a very soft and absorbed X-ray spectrum. This emission cannot be explained by either inverse Compton radiation of the compact nuclear radio source, or by an extension of the radio synchrotron emission. A comparison of the radio through X-ray energy spectrum of this source with that of bright active nuclei shows a remarkable similarity. The X-ray spectral characteristics in particular are consistent with those of the soft components present in the X-ray spectra of such objects and especially with those of the quasar PG 1211+143 (Bechtold *et al.* 1987). Applying the accretion disk model of Bechtold *et al.* to explain the soft X-ray spectrum of the nucleus of M81, we can constrain the mass of a central black hole to be $\leq 10^4 - 10^5 M_\odot$ and the accretion rate to be $\leq 10^{-4} - 10^{-3} M_\odot \text{ yr}^{-1}$.

5. The equivalent hydrogen column of the nuclear source measured in X-rays is far less than that required by an extension of the obscuration picture of Lawrence and Elvis (1982) to fainter nuclei. The simplest explanation of this is there may be a parallel sequence to the absorption picture, consisting of relatively dust-free nuclei. This is also supported by more recent results on brighter nuclei (Elvis and Lawrence 1985 and references therein).

6. There are two other relatively bright X-ray nuclear sources for which the spectral data are consistent with those of

the nucleus of M81. These are the nuclei of M33 (Trinchieri, Fabbiano, and Peres 1987) and of NGC 1313 (Fabbiano and Trinchieri 1987), which however show no other sign of activity. Although firm conclusions cannot be reached with only two objects, these two nuclei could represent a new type of source, possibly the radio-quiet counterpart of the nucleus of 3C 264, which is only prominent in X-rays (Elvis *et al.* 1981; Fabbiano *et al.* 1984).

7. Finally, the soft spectrum of the nucleus of M81, if it is typical of low-luminosity active nuclei, indicates that the contribution of these sources to the 2–10 keV X-ray background could be less than estimated by Elvis, Soltan, and Keel (1984).

I am grateful to M. Elvis for many stimulating discussions and for encouraging me to write this paper and to S. Gibbs for her thorough assistance in the data analysis and in producing overlays of the X-ray data. This work has also benefited from many conversations with G. Trinchieri during our collaboration on other aspects of the X-ray properties of normal galaxies. I thank F. Bash and M. Kaufman for kindly providing their radio map to be used in this paper and for interesting and useful conversations and comments. This work was supported under NASA grant NAS8-30751.

REFERENCES

- Bartel N., *et al.* 1982, *Ap. J.*, **262**, 556.
 Bash, F. N., and Kaufman, M. 1986, *Ap. J.*, **310**, 621.
 Bash, F. N., and Visser, H. C. D. 1981, *Astr. Ap.*, **247**, 488.
 Bechtold, J., Czerny, B., Elvis, M., Fabbiano, G., and Green, R. F. 1987, *Ap. J.*, **314**, 699.
 Beck, R., Klein, U., and Krause, M. 1985, *Astr. Ap.*, **152**, 237.
 Berkhuysen, E. M., Wielebinski, R., and Beck, R. 1983, *Astr. Ap.*, **117**, 141.
 Bertola, F., and Maffei, P. 1974, *Astr. Ap.*, **32**, 117.
 Bottinelli, L., Gouguenheim, L., Patrel, G., and de Vaucouleurs, G. 1984, *Astr. Ap. Suppl.*, **56**, 381.
 Bruzual, G. A., Peimbert, M., and Torres-Peimbert, S. 1982, *Ap. J.*, **260**, 495.
 Carleton, N. P., Elvis, M., Fabbiano, G., Willner, S. P., Lawrence, A., and Ward, M. 1987, *Ap. J.*, **318**, 595.
Cataloged Galaxies and Quasars Observed in the IRAS Survey. 1985, prepared by C. J. Lonsdale, G. Helou, J. C. Good, and W. Rice (Jet Propulsion Laboratory).
 Connolly, L. P., Mantarakis, P. Z., and Thompson, L. A. 1972, *Pub. A.S.P.*, **84**, 61.
 Crane, P. C., Giuffrida, T. S., and Carlson, J. B. 1976, *Ap. J. (Letters)*, **203**, L113.
 Czerny, B., and Czerny, M. 1986, in *Proc. Joint NASA/ESA/SERC Conf.* (ESA SP-263).
 Czerny, B., and Elvis, M. 1987, *Ap. J.*, **321**, 305.
 de Jong, T., Klein, U., Wielebinski, R., and Wunderlich, E. 1985, *Astr. Ap. (Letters)*, **147**, L6.
 de Vaucouleurs, G., de Vaucouleurs, A., and Corwin, H. G. 1976, *Second Reference Catalogue of Bright Galaxies* (Austin: University of Texas Press).
 Duric, N. 1986, *Ap. J.*, **304**, 96.
 Ellis, R. S., Gondhalekar, P. M., and Efstathiou, G. 1982, *M.N.R.A.S.*, **201**, 223.
 Elvis, M., Czerny, B., and Wilkes, B. J. 1987, in *Lecture Notes in Physics*, Vol. **226**, *The Physics of Accretion onto Compact Objects*, ed. K. O. Mason, M. G. Watson, and N. White (Berlin: Springer), p. 389.
 Elvis, M., Green, R. F., Bechtold, J., Schmidt, M., Neugebauer, G., Soifer, B. T., Matthews, K., and Fabbiano, G. 1986, *Ap. J.*, **310**, 291.
 Elvis, M., and Lawrence, A. 1985, in *Astrophysics of Active Galaxies and Quasistellar Objects*, ed. J. S. Miller (Santa Cruz: University Science Books), p. 289.
 Elvis, M., Maccacaro, T., Wilson, A., Ward, M., Penston, M., Fosbury, R. A. E., and Perola, G. C. 1978, *M.N.R.A.S.*, **183**, 129.
 Elvis, M., Soltan, A., and Keel, W. C. 1984, *Ap. J.*, **283**, 479.
 Elvis, M., and Van Speybroeck, L. 1982, *Ap. J. (Letters)*, **257**, L51.
 Elvis, M., Wilkes, B. J., and Tananbaum, H. 1985, *Ap. J.*, **292**, 357.
 Fabbiano, G. 1986, *Pub. A.S.P.*, **98**, 525.
 Fabbiano, G., Feigelson, E., and Zamorani, G. 1982, *Ap. J.*, **256**, 397.
 Fabbiano, G., Gioia, I. M., and Trinchieri, G. 1988, *Ap. J.*, **324**, 749.
 Fabbiano, G., Miller, L., Trinchieri, G., Longair, M., and Elvis, M. 1984, *Ap. J.*, **277**, 115.
 Fabbiano, G., and Trinchieri, G. 1984, *Ap. J.*, **286**, 491.
 ———. 1985, *Ap. J.*, **296**, 430.
 ———. 1987, *Ap. J.*, **315**, 46.
 Fabbiano, G., Trinchieri, G., and Macdonald, A. 1984, *Ap. J.*, **284**, 65.
 Fabbiano, G., Trinchieri, G., and Van Speybroeck, L. 1987, *Ap. J.*, **316**, 127.
 Fabricant, D., and Gorenstein, P. 1983, *Ap. J.*, **267**, 535.
 Gehrels, N. 1986, *Ap. J.*, **303**, 336.
 Gezari, D. Y., Schmitz, M., and Lee, J. 1984, NASA Ref. Pub. No. 1118.
 Giacconi, R., *et al.* 1979, *Ap. J.*, **230**, 540.
 Gioia, I. M., *et al.* 1984, *Ap. J.*, **283**, 495.
 Gorenstein, P., and Tucker, W. H. 1974, in *X-Ray Astronomy*, ed. R. Giacconi and H. Gursky (Dordrecht: Reidel), p. 267.
 Harnden, F. R., Fabricant, D. G., Harris, D. E., and Schwarz, J. 1984, Scientific Specification of the Data Analysis System for the *Einstein Observatory* (HEAO-2) IPC, Internal SAO Spec. Rept. No. 393.
 Harris, D. E., and Irwin, C. 1984, SAO/HEAD Internal Pub.
 Helou, G., Soifer, B. T., and Rowan-Robinson, M. 1985, *Ap. J. (Letters)*, **298**, L7.
 Hjellming, M., and Johnston, K. L. 1981, *Ap. J. (Letters)*, **246**, L141.
 Hummel, E. 1980, *Astr. Ap. Suppl.*, **41**, 151.
 Jenkins, E. B., and Savage, B. D. 1974, *Ap. J.*, **187**, 243.
 Kaufman, M., Bash, F. N., Kennicutt, R. C., Jr., and Hodge, P. W. 1987, preprint.
 Keel, W. C. 1983, *Ap. J. Suppl.*, **52**, 229.
 Kirschner, R. P., Oemler, A., Jr., and Schechter, P. L. 1979, *Ap. J.*, **84**, 951.
 Kriss, G. A., Canizares, C. R., and Ricker, G. 1980, *Ap. J.*, **242**, 492.
 Lawrence, A., and Elvis, M. 1982, *Ap. J.*, **253**, 410.
 Long, K. S., D'Odorico, S., Charles, P. A., and Dopita, M. A. 1981, *Ap. J. (Letters)*, **246**, L61.
 Long, K. S., Helfand, D. S., and Grabelsky, D. A. 1981, *Ap. J.*, **248**, 925.
 Long, K. S., and Van Speybroeck, L. P. 1983, in *Accretion Driven X-Ray Sources*, ed. W. Lewin and E. P. J. Van den Heuvel (Cambridge: Cambridge University Press), p. 41.
 Markert, T. H., and Rallis, A. D. 1983, *Ap. J.*, **275**, 571.
 Mauche, C. W., and Gorenstein, P. 1986, *Ap. J.*, **302**, 371.
 Miller, J. S. 1985, in *Astrophysics of Active Galaxies and Quasi-stellar Objects*, ed. J. S. Miller (Santa Cruz: University Science Books), p. 367.
 Mushotzky, R. F. 1984, in *Proc. X-Ray and UV Emission from Active Galactic Nuclei*, ed. W. Brinkmann (Garching: Max-Planck-Institut), p. 73.
 Mushotzky, R. F., Marshall, R. E., Boldt, E. A., Holt, S. S., and Serlemitsos, P. J. 1980, *Ap. J.*, **235**, 377.
 O'Connell, R. W. 1983, *Ap. J.*, **267**, 80.
 Palumbo, G. G. C., Fabbiano, G., Fransson, C., and Trinchieri, G. 1985, *Ap. J.*, **298**, 259.
 Peimbert, M., and Torres-Peimbert, S. 1981, *Ap. J.*, **245**, 845.
 Persson, C. J., and Helou, G. 1987, *Ap. J.*, **314**, 513.
 Reichert, G. A., Mushotzky, R. F., Petre, R., and Holt, S. S. 1985, *Ap. J.*, **296**, 69.
 Rickard, L. J., and Harvey, P. M. 1984, *A.J.*, **89**, 1520.
 Roberts, W. W., Roberts, M. S., and Shu, F. H. 1974, *Ap. J.*, **196**, 381.
 Rogers, A. E. E., Whitney, A. R., Cappallo, R. J., Graham, D. A., Romney, J. D., and Preston, R. A. 1982, *Ap. J.*, **262**, 556.
 Samorski, M., and Stamm, W. 1983, *Ap. J. (Letters)*, **268**, L17.
 Sandage, A. 1961, *The Hubble Atlas of Galaxies* (Carnegie Inst. Pub. No. 618).
 ———. 1984, *A.J.*, **89**, 621.
 Sandage, A., and Tamman, G. A. 1981, *A Revised Shapley-Ames Catalog of Bright Galaxies* (Carnegie Inst. Pub. No. 635).
 Schweizer, F. 1976, *Ap. J. Suppl.*, **31**, 313.
 Seward, F. D., and Mitchell, M. 1981, *Ap. J.*, **243**, 736.
 Shuder, J. M., and Osterbrock, D. E. 1981, *Ap. J.*, **250**, 55.
 Stark, A. A., Heiles, C., Bally, J., and Linke, R. 1984, in preparation.
 Trinchieri, G., Fabbiano, G., and Canizares, C. R. 1986, *Ap. J.*, **310**, 637.
 Trinchieri, G., Fabbiano, G., and Palumbo, G. G. C. 1985, *Ap. J.*, **290**, 96.
 Trinchieri, G., Fabbiano, G., and Peres, G. 1988, *Ap. J.*, **325**, 531.
 van den Bergh, S. 1959, *Pub. David Dunlop Obs.*, **2**, 147.
 van den Heuvel, E. P. J. 1980, in *X-Ray Astronomy, Proc. NATO Adv. Study Institute*, p. 119.
 Van Speybroeck, L., Epstein, A., Forman, W., Giacconi, R., Jones, C., Liller, W., and Smarr, L. 1979, *Ap. J. (Letters)*, **55**, L45.
 Visser, H. C. D. 1980a, *Astr. Ap.*, **88**, 149.
 ———. 1980b, *Astr. Ap.*, **88**, 159.
 von Kapp-her, A., Berkhuysen, E. M., and Wielebinski, R. 1978, *Astr. Ap.*, **62**, 51.
 Ward, M., Elvis, M., Fabbiano, G., Carleton, N. P., Willner, S. P., and Lawrence, A. 1987, *Ap. J.*, in press.
 Watson, M. G., Willingale, R., Grindlay, J. E., and Seward, F. D. 1983, *Ap. J.*, **273**, 688.
 Watson, M. G., Stanger, V., and Griffiths, R. E. 1984, *Ap. J.*, **286**, 144.
 Wilkes, B. J., and Elvis, M. 1987, *Ap. J.*, **323**, 243.